Journal of Medicinal Chemistry

Article

pubs.acs.org/jmc

Development and in Vitro Evaluation of a Microbicide Gel Formulation for a Novel Non-Nucleoside Reverse Transcriptase Inhibitor Belonging to the *N*-Dihydroalkyloxybenzyloxopyrimidines (N-DABOs) Family

Cristina Tintori,[†] Annalaura Brai,[†] Maria Chiara Dasso Lang,[†] Davide Deodato,[†] Antonia Michela Greco,[†] Bruno Mattia Bizzarri,[†] Lorena Cascone,[†] Alexandru Casian,[†] Claudio Zamperini,[†] Elena Dreassi,[†] Emmanuele Crespan,[‡] Giovanni Maga,[‡] Guido Vanham,[§] Elisa Ceresola,[⊥] Filippo Canducci,[⊥] Kevin K. Ariën,[§] and Maurizio Botta*[,†,∥]

[†]Dipartimento Biotecnologie, Chimica e Farmacia, Università degli Studi di Siena, Via A. De Gasperi 2, I-53100 Siena, Italy

[‡]Istituto di Genetica Molecolare, IGM-CNR, Via Abbiategrasso 207, I-27100 Pavia, Italy

[§]Virology Unit, Institute of Tropical Medicine, Nationalestraat 155, B-2000 Antwerpen, Belgium

[∥]Biotechnology College of Science and Technology, Temple University, Biolife Science Building, Suite 333, 1900 N 12th Street, Philadelphia, Pennsylvania 19122, United States

[⊥]Department of Biotechnology and Life Sciences, University of Insubria, Dunant 3, 21100, Varese, Italy

Supporting Information

ABSTRACT: Preventing HIV transmission by the use of a vaginal microbicide is a topic of considerable interest in the fight against AIDS. Both a potent anti-HIV agent and an efficient formulation are required to develop a successful microbicide. In this regard, molecules able to inhibit the HIV replication before the integration of the viral DNA into the genetic material of the host cells, such as entry inhibitors or reverse transcriptase inhibitors (RTIs), are ideal candidates for prevention purpose. Among RTIs, *S*- and *N*-dihydroalkyloxybenzyloxopyrimidines (S-DABOs and N-DABOs) are interesting compounds active at nanomolar concentration against wild type of RT and with a very interesting activity against RT mutations. Herein, novel N-DABOs were synthesized and tested as anti-HIV agents. Furthermore, their mode of binding was studied by molecular modeling. At the same time, a vaginal microbicide gel formulation was developed and tested for one of the most promising candidates.

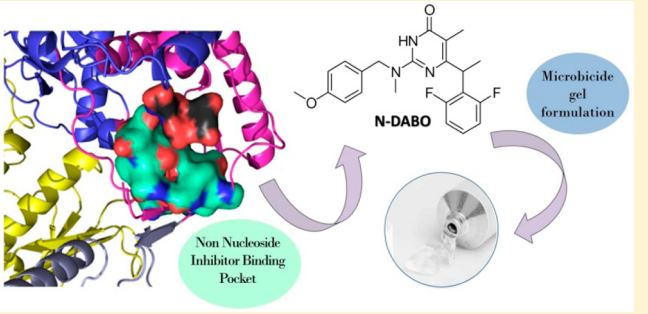

INTRODUCTION

Since its discovery in 1981, human immunodeficiency virus (HIV) infection continues to be a major health threat worldwide. Combination antiretroviral therapy (cART) can significantly reduce the viral load and prolong patients' life expectancy, but it is not able to totally eradicate the virus.[1] Furthermore, the emergence of resistant strains continues to limit the efficacy of current drugs.[2] Accordingly, a great variety of chemotherapy agents were developed against HIV-1 in the past 20 years. Most of the anti-HIV studied small-molecules target the viral enzyme reverse transcriptase (RT) by binding the polymerase active site (nucleoside RT inhibitors) or an allosteric pocket (non-nucleoside RT inhibitors or NNRTIs).[3,4] More than 30 different molecular structures of NNRTIs were developed, comprising nevirapine, delavirdine, efavirenz, rilpivirine, and etravirine FDA-approved drugs. Among NNRTIs, *S*- and *N*-dihydroalkylthiobenzyloxopyrimidines (S-DABOs and N-DABOs) have been extensively modified by our research group with the aim of improving their inhibitory activity toward RT wild-type and clinically relevant mutants.[5−13] Several compounds showed nanomolar inhibitory potency against wild-type HIV-1 and relevant drug-resistant mutants. Furthermore, previous studies revealed that the conversion of the S-DABO derivatives into the corresponding N-DABOs may lead to new derivatives characterized by improved ADME profiles, especially aqueous solubility (Chart 1).[13] On the other hand, HIV transmission remains high in developing countries, and with a vaccine not yet in sight, the development of an effective prevention strategy would be desirable. Topical microbicides are preparations able to prevent the transmission of HIV when applied to the genital and/or

Received: December 22, 2015

DOI: 10.1021/acs.jmedchem.5b01979
J. Med. Chem. XXXX, XXX, XXX−XXX

Chart 1. Hit Compounds Belonging to S-DABO and N-DABO Families

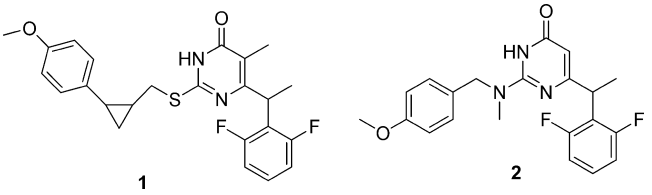

1 2

lower gastrointestinal graft via the rectum.[14] It is generally accepted that a microbicide should act prior to the integration of proviral DNA into the host cell DNA. Accordingly, the two main compound classes that could be used to such a purpose are entry inhibitors and RT inhibitors. Examples of RT inhibitors in preclinical and clinical evaluation as microbicides include tenofovir, dapivirine, MIV150, UC781, UAMC01398, and DABO.[15−20] Microbicide candidates must have a good selectivity index (SI), inhibit virus replication at low, nontoxic concentrations in vitro, have a good resistance profile, be stable, and have the potential for reasonable pricing.[21−24] In this context, the purpose of this work was to initiate a study on N-DABO NNRTIs in order to investigate their potential for the development of new microbicides. To this aim, a novel series of N-DABO derivatives was synthesized. Biological evaluation showed that these compounds are able to inhibit HIV-1 replication at nanomolar concentration. Remarkably, the most promising derivative in terms of activity against mutant strains, **25e**, was also characterized by a high selectivity index, 5-fold higher than dapivirine, a good cell permeability, and stability higher than 95%. On this basis, a vaginal microbicide gel formulation of **25e** was developed and evaluated in vitro. Moreover, in the present work we also reported the development of a predictive QSAR model for a large set of S-DABO/N-DABO derivatives.

RESULTS AND DISCUSSION

Chemistry. The new compounds were synthesized using the classical approach for the synthesis of N-DABO, based on the nucleophilic displacement of the methylsulfonyl group at C2 position with the appropriate amine. According to Scheme 1, the key intermediates **13** and **14** were synthesized starting from the appropriate carboxylic acids (**3** and **4**) that were methylated with MeI using LDA as a base to obtain compounds **5** and **6** in good yields, while compound **12** was synthesized directly from acid **4**.

The β-ketoesters **9**−**11** were prepared by activation of acids **4**−**6** using 1,1′-carbonyldiimidazole (CDI), followed by treatment with potassium monoethyl malonate **8** in the presence of anhydrous $MgCl_2$ and Et_3N. Then condensation of **9**−**11** with thiourea in the presence of EtONa led to substituted thiouracils **12**−**14**. Subsequent alkylation with MeI in DMF gave compounds **15**−**17** in excellent yield. C2-methylthio group of thiouracils **15**−**17** was then converted in the corresponding sulfone derivatives **18**−**20**, by oxidation.

Secondary amines **22b**−**g** were synthesized by reductive amination of the appropriate aldehyde (**21b**−**g**) with methylamine and sodiumborohydride. Nucleophilic substitution of the C2-methylsulfonyl group of **18**−**20** with the appropriate amine led to final compounds **23a**−**f**, **24a**, **24c**−**f**, and **25d**−**g** (Scheme 2). Boc deprotection of compounds **23b** and **24b** led to compounds **23a** and **24a** (Scheme 3).

Aldehydes **21b**−**d** were not commercially available and were synthesized by nucleophilic displacement of the 4-fluorobenzaldehyde with the appropriate amine (Scheme 4).

Biology. Antiviral Activity against HIV-1 and Cytotoxicity. Compounds **23a**−**f**, **24a**, **24c**−**f**, and **25d**−**g** were

Scheme 1[a]

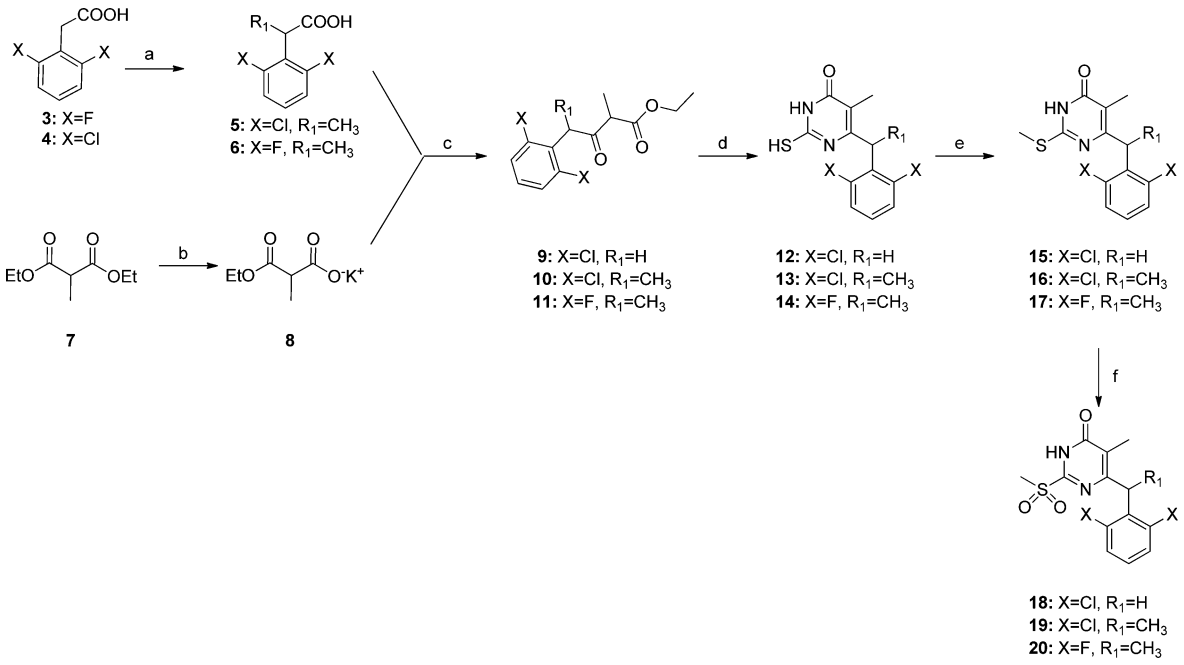

[a]Reagents and conditions: (a) LDA, HMPA, CH_3I, dry THF, −78 °C to rt, 12 h; (b) KOH, dry EtOH, 0 °C to rt, 12 h; (c) carbonyldiimidazole, $MgCl_2$, TEA, dry CH_3CN, rt, 12 h; (d) Na^0, thiourea, dry EtOH, reflux, 12 h; (e) CH_3I, KOH, EtOH, rt, 1 h; (f) m-CPBA, dry DCM, 0 °C to rt, 12 h.

DOI: 10.1021/acs.jmedchem.5b01979
J. Med. Chem. XXXX, XXX, XXX−XXX

Scheme 2[a]

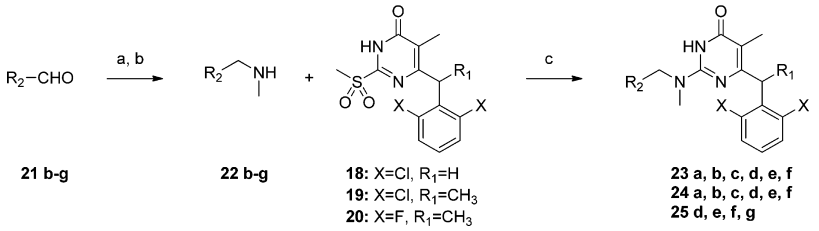

[a]Reagents and conditions: (a) $MeNH_2$, $NaHCO_3$, MeOH, reflux 4 h; (b) $NaBH_4$, 0 °C to rt, 1 h; (c) dry toluene, reflux, 48 h.

Scheme 3[a]

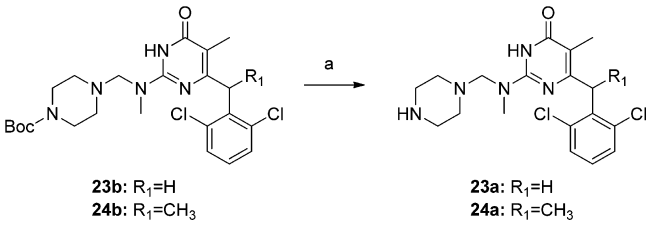

[a]Reagents and conditions: (a) 10% TFA in dry DCM, rt 1 h.

Scheme 4[a]

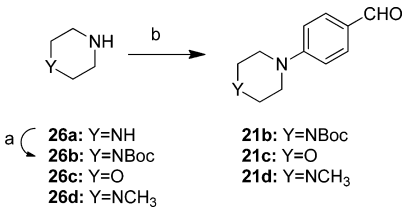

[a]Reagents and conditions: (a) di-*tert*-butyl dicarbonate, MeOH, microwave, 2 min; (b) 4-fluorobenzaldehyde, K_2CO_3, dry DMF, 130 °C, 12 h.

evaluated for their anti-HIV-1 activity and cytotoxicity in TZM-bl cells in comparison with TMC120 (dapivirine). The results, expressed as EC_{50} (50% effective concentration), CC_{50} (50% cytotoxic concentration), and SI (selectivity index given by the CC_{50}/EC_{50} ratio) values are summarized in Table 1. Among the novel N-DABOs, compounds **23e**, **23f**, **24e**, **24d**, **25d**, **25e**, and **25f** retained an activity similar to that of the lead **1** and showed very potent inhibitory activities against the replication of the V106A[25] mutant virus which is resistant to nevirapine (Table 2). On the other hand, the compounds were also active at nanomolar concentration against V90I, V106A, E138K, and K101E mutants while modestly active against the L100I, K103N, and Y181C[25] mutants. Moderate activities against WT RT were found for derivatives **23d**, **24a**, and **24c**. Remarkably, the most active compounds also showed low cytotoxicity and resulting high selectivity indices, with the best compound, **25e**, characterized by SI higher than 10 000. This feature together with the good activity profile makes this compound suitable for microbicide formulation.

Antireverse Transcriptase Activity. Compounds **23c**, **23e**, **23f**, and **24e** were further evaluated for antireverse transcriptase activity in comparison with nevirapine in an enzymatic recombinant HIV-1 RT activity assay, and results expressed as IC_{50} were compared with anti-HIV-1 activity. Comparable activity values were found, confirming that the target of these antiviral agents is the RT and that compounds are able to permeate through the cellular membrane, inhibit RT, and subsequently block the HIV-1 replication.

Antiviral Activity for 25e Gel. Antiviral activity testing was performed with a gel formulation of **25e** in direct comparison with the free drug and the blank gel. As measured in TZM-bl cells, the EC_{50} values of formulated and native **25e** are similar, which indicates that formulating **25e** does not alter the in vitro potency of the compound (Figure 1a). In addition, no loss in antiviral activity was observed for the **25e** gel formulation after storage for 1 month at room temperature and without light exposure.

To exclude the effect of β-cyclodextrins on the observed antiviral activity and the toxicity of these gels in vitro even at low gel concentrations (toxicity was observed at 5% gel concentration), gels were reformulated without β-cyclodextrins. Moreover, to reproduce more physiological conditions, TZM-bl cells were seeded into Transwells and the gel was applied onto the cell monolayer at 50% fixed concentration with serial drug (**25e** or tenofovir) dilutions. This experiment confirmed the high antiviral activity of **25e** gel (EC_{50} = 30 nM) also in comparison with the observed efficacy of tenofovir gel (EC_{50} = 3 μM) (Figure 1b).

In Vitro ADME Studies. Selected N-DABOs were profiled in vitro for aqueous solubility at pH 4.2 and 7.4, liver microsomal stability, and membrane permeability (Table 3). Their aqueous solubility (−log *S* ranging from −6.51 to −8.60 and from −5.49 to −7.99 at pH 7.4 and 4.2, respectively), although improved over the S-DABOs previously developed, was rather low. This aspect does not prevent the efficacy of the gel formulation which is composed of cyclodextrins, commonly used to increase drug solubility.[26,27] Furthermore, cyclodextrins have been shown to determine a dose-dependent inactivation of the virus by the removal of cholesterol from the membrane of HIV-infected cells, thus enhancing the infection prevention of the microbicide formulation. On the other hand, passive membrane permeability in a PAMPA assay indicated acceptable cell permeability values for compound **25e** (5.54 and 3.78 × 10^{-6} cm/s, at pH 4.2 and 7.4, respectively). Moreover, stability tests disclosed that all analogues showed excellent metabolic stability in liver microsomes (~99%).

Stability of 25e Gel Formulation. **25e** gel (85% of compound was loaded that corresponded with a final concentration of 17 μM) at pH 4.2 (vaginal formulation) was found to be stable at room temperature without light exposure: the **25e** recovery after 1 month of storage amounted to about 100%. In addition, the viscosity and pH of this gel remained stable during storage.

Molecular Modeling. Docking Studies. Docking studies have been previously used to characterize the binding mode of S-DABOs within the non-nucleoside binding pocket of RT wild type.[11,12] A schematic representation of the main interactions

DOI: 10.1021/acs.jmedchem.5b01979
J. Med. Chem. XXXX, XXX, XXX−XXX

Table 1. Antienzymatic Activity, Antiviral Activity, and Cytotoxicity of the New N-DABO Derivatives

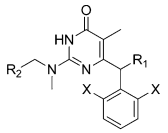

Name	R_2	R_1	X	Antiviral activity against WT HIV-1 EC_{50} (nM)[a]	Enzymatic anti-RT activity IC_{50} (nM)[a]	CC_{50} (μM)
23a	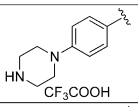	H	Cl	110.0	ND[b]	20.7
23b	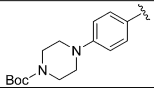	H	Cl	2933.0	ND	2.59
23c	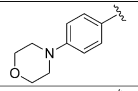	H	Cl	657.0	90.0	9.9
23d	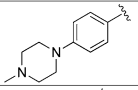	H	Cl	94.0	ND	3.2
23e	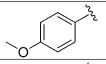	H	Cl	**15.0**	**5.0**	17.9
23f	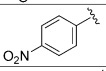	H	Cl	**8.6**	**7.85**	19.5
24a	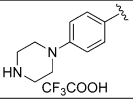	Me	Cl	102.0	ND	13.2
24c	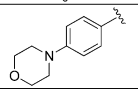	Me	Cl	86.0	ND	38.4
24d	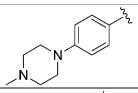	Me	Cl	**32.0**	ND	>10.0
24e	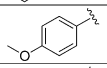	Me	Cl	**12.0**	**17.0**	>100.0
24f	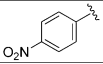	Me	Cl	104	ND	>50.0
25d	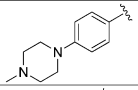	Me	F	**7.9**	ND	26.2
25e	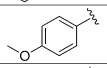	Me	F	**3.3**	ND	88.8
25f	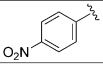	Me	F	**10.0**	ND	>50.0
25g	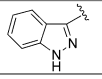	Me	F	329.0	ND	>100.0
1				93.0	ND	31.1
2				2.6	ND	48.1
Dapivirine				**1.3**	ND	**3.4**
Nevirapine				**ND**	125	**ND**

[a]Data represent the mean of at least two experiments. [b]ND: not determined.

Table 2. Anti-HIV Activities of Selected Compounds against Mutant Strains[a]

compd	EC_{50} (nM) pNL4.3 WT	V90I (nM)	L100I (nM)	E138 K (nM)	K101E (nM)	K103N (nM)	V106A (nM)	Y181C (nM)
23d	100	ND	ND	274	>1000	792	18	704
23e	15	ND	ND	ND	ND	ND	10	680
23f	8.6	13	220	35	51	367	ND	201
24c	96	ND	ND	256	942	1502	15	1288
24d	29	ND	ND	103	294	1039	6.3	627
24e	12	ND	ND	ND	ND	ND	10	209
25d	7.9	22	1570	42	138	2460	ND	331
25e	**5**	**8.7**	**84**	**17**	**31**	**102**	ND	**80**
25f	10	30	1498	65	134	518	ND	814
25g	329	687	>10000	950	>10000	>10000	ND	>10000
1	93	ND	ND	246	450	549	56	1608
2	3	ND	ND	9.1	17	34	0.87	94

[a]All these viruses are site-directed mutants. pNL4.3 replication competent viruses with single point mutations introduced in HIV RT by site-directed mutagenesis.

established by S-DABOs is reported in Figure 2. Two hydrogen bonds were detected between the amide moiety of the pyrimidinone ring and the backbone of Lys101. The C6-benzyl group established hydrophobic interactions with the aromatic cage formed by Tyr181, Tyr188, Phe227, Trp229, and Leu100, while the C6′-group interacted with Val179. Finally profitable lipophilic interactions were found between the S side chain and a solvent-exposed channel lined by residues Val106, Pro225, Tyr318, Phe227, and Pro236.

Herein, molecular docking simulations were conducted on new N-DABOs following the computational protocol previously adopted on S-DABOs. Besides Autodock,[28] two more software programs were used, namely, Gold[29] and Glide,[30,31] and the three computational procedures were extended to a large set of compounds including 168 S-DABOs/N-DABOs[11−13,32,33] characterized by IC_{50} values ranging from 0.0003 and 50 μM against RT wt (Table S1, Supporting Information). In parallel, the same docking analyses were conducted by considering a well-ordered water molecule crystallized into the binding pocket of 1RT2 crystal structure, which forms a triad of hydrogen bonds involving the inhibitor, the main chain nitrogen of Lys101, and a carboxyl oxygen of

DOI: 10.1021/acs.jmedchem.5b01979
J. Med. Chem. XXXX, XXX, XXX−XXX

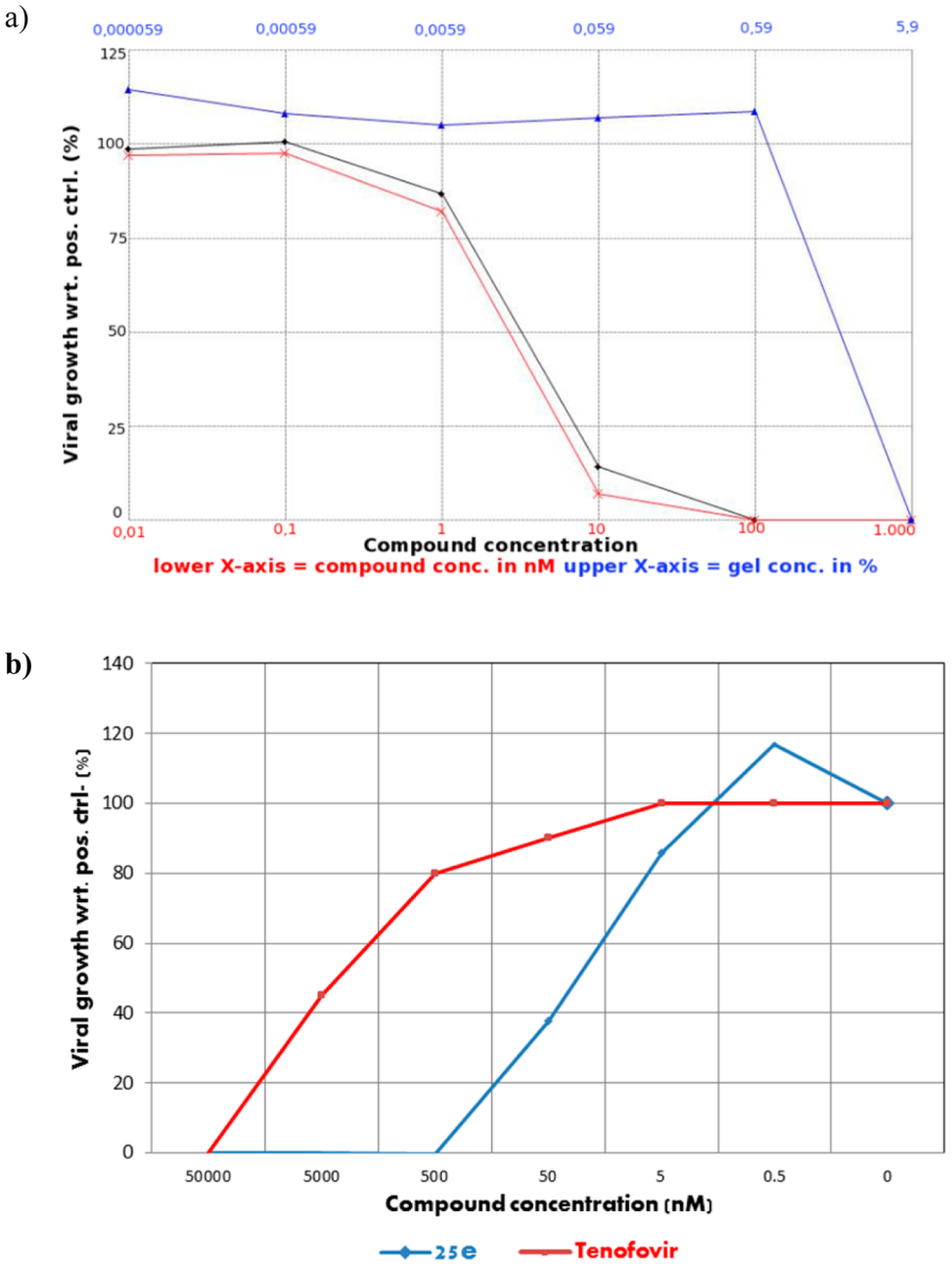

Figure 1. Anti-HIV activity of **25e** (black line) and **25e** gel (red line) in human Tzm-Bl. (a) The EC_{50} values for the free drug and the gel formulation were similar, ranging from 2.3 to 3.3 nM, respectively. Each concentration was evaluated in triplicate. Toxicity was evaluated in parallel, and the blank gel showed toxicity at a concentration higher than 100 nM. (b) The EC_{50} was evaluated by Transwell assays and without β-cyclodextrins in the gel formulation. The usage of Transwells has allowed use of the gels at a 50% fixed concentration at all dug dilutions with no toxicity on the cells. Tenofovir was used as control.

Table 3. In Vitro ADME Profile of N-DADO Derivatives

compd	PAMPA, pH 7.4 (10^{-6} cm/s)	PAMPA, pH 4.2 (10^{-6} cm/s)	water solubility, pH 7.4 (log S)[a]	water solubility, pH 4.2 (log S)[a]	metabolic stability (%)[b]
23c	21.9	ND	−8.6	−7.80	99
23d	1.37	0.58	−6.51	−5.49	99
24d	0.91	ND	−8.7	−7.85	99
23f	10.93	1.90	−7.55	−6.70	99
25e	5.54	3.78	−8.60	−7.99	99

[a]log S = log mol L^{-1}. [b]Expressed as percentage of unmodified parent drug.

Glu138 in the p51 chain. Remarkably, the three software programs converged to the same solution in both the presence and absence of the water molecule and the poses obtained for N-DABOs perfectly overlapped with those of S-DABOs derivatives previously reported. As an example, Figure 3 shows the binding mode of compound **24e** aligned with the congeneric S-DABO.

Although coincident poses were obtained through the use of different docking procedures which made the results highly confident, no correlation was found between the scoring functions employed (Glide SP and XP, Autodock, ChemScore) and the experimental activity values. Bad results were also obtained through pose rescoring by X-Score[34] (an empirical

DOI: 10.1021/acs.jmedchem.5b01979
J. Med. Chem. XXXX, XXX, XXX−XXX

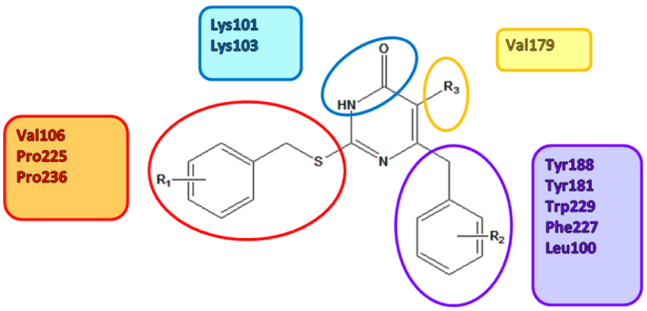

Figure 2. Binding mode of S-DABOs within the NNBP of RT wt (PDB code 1RT2) as previously predicted by docking studies through the Autodock software.

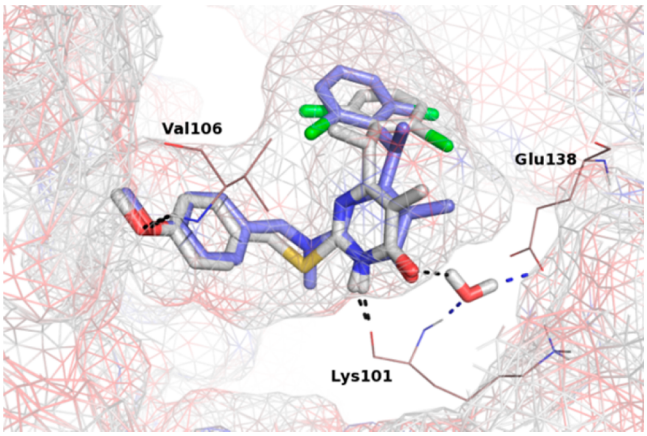

Figure 3. Binding mode of compound **24e** (sky blue stick) within the NNBP of RT. For comparison purposes, the congeneric S-DABO (gray stick) is also visualized. For the sake of clarity, only a few key residues are labeled, hydrogen atoms are omitted, and hydrogen-bonding interactions are represented by black dashed lines.

scoring function) and MM-GBSA[35] (a force field based function) methods. This was not surprising and was also recently found for another family of NNRTIs.[36] In order to derive a quantitative structure−activity relationship, the new N-DABO derivatives together with additional N-DABOs and S-DABOs previously described by us[11,13] and other research groups[32,33] were submitted to a multiple linear regression (MLR) analysis with the aim of identifying the molecular determinants able to influence their activity against wild type HIV-1. For this purpose, the MLR algorithm implemented in Canvas was applied. In particular, 68 compounds with activity data spanning over 6 orders of magnitude were used as learning set. Several models were generated by using the cellular data (EC_{50}) as the independent variable, 87 descriptors as dependent variables, and choosing in turn an increasing number of X variables as best subset. Besides the parameters coming from docking studies, 2D fingerprint descriptors and QikProp properties were calculated. The learning set (the first 68 compounds in Table 1S) was randomly divided into a training set (80%) and a test set (20%). A good predictive ability, both internal and external, was found with an equation characterized by seven descriptors: evdw (van der Waals energy calculated by Glide during the docking with water), PISA (π, carbon, and attached hydrogen, component of the SASA), three prime descriptors[37,38] (prime mmgbsa bind lipo, prime mmgbsa DG bind, primesolv GB), HPScore,[34] dendritic (2D fingerprint).[39] Equation was assessed by both internal and external validation procedures. Good r^2 (0.76) and leave-three-out cross-validated correlation coefficients q^2 (0.72) were found (Figure 4). We decided to stop our analysis to seven properties because increasing the number of descriptors, even to determine an improvement of the predictive power of the model on the training set, led to bad q^2 values on the external test set. Remarkably, the 68 compounds belonging to the learning set were extracted from the larger original database of 168 derivatives on the basis of a solubility criteria (QPLogS < −6.0). Indeed, because of their scarce solubility, some

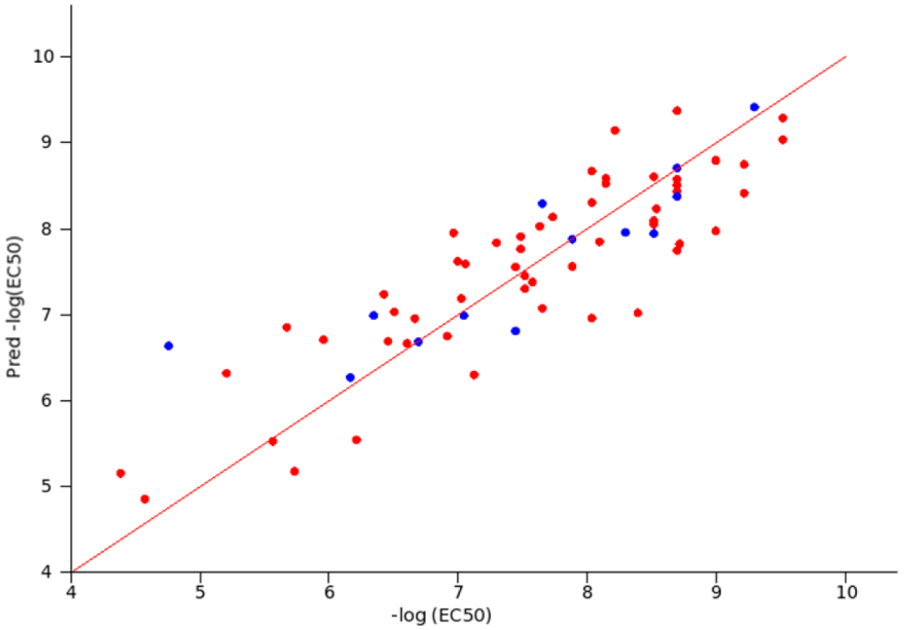

Figure 4. Experimental activity (−log EC_{50}) versus predicted activity (Pred −log(EC_{50})) in the final MLR model. Red points represent prediction for the training set, while blue points represent predictions for the test set.

DOI: 10.1021/acs.jmedchem.5b01979
J. Med. Chem. XXXX, XXX, XXX−XXX

derivatives tended to precipitate from medium, and their activity values were thus underestimated. Accordingly, the models generated including all compounds were characterized by lower r^2 values ($r^2 < 0.5$, data not shown). Overall, this study suggests that docking scoring functions are poor in predicting the activity of DABO derivatives against RT. However, a regression model combining docking results with other 2D descriptors gives the possibility to obtain more accurate prediction. The model generated herein could be exploited for the design of new S-DABO/N-DABO RT inhibitors taking into due consideration that the application domain of this QSAR model is limited to compounds with QPLogS < −6.0.

CONCLUSIONS

N-DABOs, which previously appeared to be very potent against HIV-1 with a good activity against NNRTI-resistant viruses, also proved to have an excellent cellular safety profile and to possess pharmacokinetic characteristics that make them promising microbicide gels to be used for HIV prevention. This family of RT inhibitors was further explored herein by the synthesis and biological evaluation of new derivatives. Among them, **25e** was chosen to be formulated because of its good activity profile and high selectivity index (>17 000), an important feature for the development of an effective topical microbicide. The gel formulation has been shown to be stable and effective against HIV-1 replication. Remarkably, **25e** formulated in gel form demonstrated ability in treating HIV-1 infection comparable to that of the free drug. Overall, results reported herein support the anti-HIV microbicide potential of N-DABO RT inhibitors.

EXPERIMENTAL SECTION

Methods. All commercially available chemicals were used as purchased. DCM and CH_3CN were dried over sodium hydride. EtOH was dried over Mg. THF and toluene solvents were dried over Na/benzophenone prior to use. Anhydrous DMF was used as purchased. Anhydrous reactions were run under a positive pressure of dry N_2 or Ar.

Instrumentation. ^{1}H NMR and ^{13}C NMR spectra were measured on a 400 and 100 MHz spectrometer, respectively. Chemical shifts for protons are reported in parts per million (δ scale) and internally referenced to the $CDCl_3$ signal at δ 7.24 ppm, to the DMSO at δ 2.50 ppm, and to the D_2O signal at δ 4.79 ppm. Chemical shifts for carbon are reported in parts per million (δ scale) and referenced to the carbon resonances of the solvent ($CDCl_3$: δ 77.76 ppm, the middle peak). Data are presented as follows: chemical shift, multiplicity (s = singlet, d = doublet, dd = double doublet, td = triple doublet, t = triplet, q = quartet, m = multiplet and/or multiplet resonances, br = broad), coupling constant in hertz (Hz), and integration. The purity of compounds was assessed by reverse phase liquid chromatography and a mass spectrometer with a UV detector at λ= 254 nm and an electrospray ionization source (ESI). All the solvents were HPLC grade. Mass spectral (MS) data were obtained using a LC/MSD VL system with a 0.4 mL/min flow rate using a binary solvent system of 95:5 methanol/water. UV detection was monitored at 254 nm. Mass spectra were acquired in positive or negative mode scanning over the mass range of 100−1500. The following ion source parameters were used: drying gas flow, 9 mL/min; nebulize pressure, 40 psig; drying gas temperature, 350 °C. Microwave reactions were conducted using a CEM Discover synthesis unit (CEM Corp., Matthews, NC). The machine consists of a continuous focused microwave power delivery system with operator-selectable power output from 0 to 300 W. The temperature of the contents of the vessel was monitored using a calibrated infrared temperature control mounted under the reaction vessel. All experiments were performed using a stirring option whereby the contents of the vessel are stirred by means of a rotating magnetic plate located below the microwave cavity and a Teflon-coated magnetic stir bar in the vessel.

Chromatographic analysis was performed using a Varian Polaris 5 C18-A column (150 mm × 4.6 mm, 5 μm particle size) at room temperature. Analysis was carried out using gradient elution of a binary solution; eluent A was ACN, while eluent B consisted of water. The analysis started at 0% A for 3 min, then rapidly increased up to 98% in 12 min, and finally remained at 98% A until 18 min. The analysis was performed at flow rate of 0.8 mL min^{-1}, and injection volume was 20 μL. Purity of compounds (as measured by peak area ratio) was >95%.

Chemistry. General Procedure for the Preparation of 2-(2,6-Dihalophenyl)alkanoic Acids (5 and 6). Spectroscopic and analytical data for compounds are in agreement with those reported in the literature.

Example: 2-(2,6-Difluorophenyl)propanoic Acid 6[40]. A 1.6 M solution of *n*-butyllithium in hexane (8.35 mL, 13.4 mmol) was added dropwise in a round-bottomed flask charged with a magnetic stirrer and diisopropylamine (1.87 mL, 13.4 mmol), under anhydrous conditions at −78 °C. After 15 min the mixture was diluted with dry THF (16 mL) and stirred at −78 °C for further 30 min. A solution of the appropriate acid (1.00 g, 5.8 mmol) in dry THF (14 mL) and HMPA (1.52 mL, 8.7 mmol) were added dropwise, and the mixture was warmed to −10 °C and stirred for 30 min. The orange solution obtained was cooled to −78 °C, iodomethane (0.54 mL, 8.7 mmol) was added, and the colorless solution obtained was gently warmed to room temperature and stirred for 12 h. The mixture was then treated with HCl 1 N (100 mL) and extracted with EtOAc (3 × 100 mL). The combined organic phases were washed with HCl 1 N and brine, dried over Na_2SO_4, filtered, and concentrated under reduced pressure. The crude residue was purified by flash chromatography on silica gel, eluting with 25% DCM/EtOAc to give pure compound **6** (isolated yield 92%). ^{1}H NMR (400 MHz, $CDCl_3$) δ ppm 11.10 (bs, 1H) 7.32−7.12 (m, 1H), 6.98−6.80 (m, 2H), 4.15 (q, J = 7.3 Hz, 2H), 1.50 (t, J = 16.1 Hz, 3H). LRMS (ESI) m/z = 184 $[M - H]^-$.

2-(2,6-Dichlorophenyl)propanoic Acid 5. ^{1}H NMR (400 MHz, $CDCl_3$) δ ppm 11.73 (bs, 1H) 7.32−7.28 (m, 1H), 7.13 (t, J = 8.0 Hz, 2H), 4.58 (q, J = 7.2 Hz, 1H), 1.54 (d, J = 7.2 Hz, 3H). LRMS (ESI) m/z = 218 $[M - H]^-$.[40]

Potassium 3-Ethoxy-2-methyl-3-oxopropanoate 8. A stirred solution of diethyl methylmalonate (2.00 g, 11.5 mmol) in dry EtOH (7 mL) under Ar atmosphere was cooled to 0 °C, and a solution of KOH (0.64 g, 11.5 mmol) in dry EtOH (7 mL) was added dropwise. The mixture was stirred at 0 °C for 30 min and then at room temperature for 12 h. Solvent was evaporated, and the residue was triturated with DCM. The white solid obtained was filtered, washed with hexane, and used in the next step without further purification (isolated yield 56%). ^{1}H NMR (400 MHz D_2O) δ ppm 4.11 (q, J = 7.1 Hz, 2H), 3.29 (q, J = 7.2 Hz, 1H), 1.24 (d, J = 7.2 Hz, 3H), 1.19 (t, J = 7.1 Hz, 3H).

General Procedure for the Preparation of Ethyl 4-(2,6-Dihalophenyl)-2-methyl-3-oxoalkanoates (9−11). Example: 4-(2,6-Difluorophenyl)-2-methyl-3-oxopentanoate 11. To stirred solution of **8** (1.59 g, 8.6 mmol) in dry CH_3CN (20 mL) under argon atmosphere triethylamine (1.66 mL, 12.0 mmol) and magnesium chloride (0.85 g, 8.9 mmol) were added. The mixture was stirred at room temperature for 1 h, and then a solution of **6** (0.51 g, 2.8 mmol) and carbonyldiimidazole (0.50 g, 3.0 mmol) in dry CH_3CN (15 mL) was added dropwise. The mixture was stirred at room temperature for 12 h, then refluxed for 2 h. After cooling, the mixture was gently treated with HCl 3 N (20 mL) and the layers were separated. The organic phase was washed with brine and a saturated solution of $NaHCO_3$ (3 × 20 mL). The organic solution was dried over Na_2SO_4, filtered, and concentrated under reduce pressure. The crude residue was purified by flash chromatography on silica gel, eluting with 10% EtOAc/Hex to give pure compound **11** (isolated yield 61%). ^{1}H NMR (400 MHz, $CDCl_3$) δ ppm 7.22−7.19 (m, 1H), 6.90−6.84 (m, 2H), 4.15 (dq, J = 7.2 Hz, 2H), 4.08−4.05 (m, 1H), 3.47−3.38 (m, 1H) 1.38 (t, J = 17.6 Hz, 3H), 1.29−1.22 (m, 6H). ^{13}C NMR (100 MHz, $CDCl_3$) δ ppm 203.67, 170.13, 162.24, 129.21, 11.80, 111.69, 111.55,

DOI: 10.1021/acs.jmedchem.5b01979
J. Med. Chem. XXXX, XXX, XXX−XXX

111.43, 61.16, 49.94, 46.04, 41.40, 14.76, 13.61, 12.7. LRMS (ESI) m/z = 293 $[M + H]^+$.

Ethyl 4-(2,6-Dichlorophenyl)-2-methyl-3-oxobutanoate 9. ^{1}H NMR (400 MHz, $CDCl_3$) δ ppm 7.29 (d, J = 8.0 Hz, 2H), 7.11−7.09(m, 1H), 4.30 (s, 2H), 4.20 (q, J = 7.2 Hz, 2H), 3.68 (q, J = 7.4 Hz, 1H), 1.41(d, J = 7.1 Hz, 3H), 1.29 (t, 3H). LRMS (ESI) m/z = 290 $[M + H]^+$.

Ethyl 4-(2,6-Dichlorophenyl)-2-methyl-3-oxopentanoate 10. ^{1}H NMR (400 MHz, $CDCl_3$) δ ppm 7.33(d, J = 8.0 Hz, 2H), 7.20−7.15 (m, 2H), 4.61 (q, J = 7.2 Hz, 1H), 4.09 (q, J = 6.2 Hz, 2H), 3.45 (q, J = 5.2 Hz, 1H), 1.45 (d, J = 7.2 Hz, 3H), 1.29 (d, J = 5.2 Hz, 3H), 1.22 (t, J = 6.2 Hz, 3H). LRMS (ESI) m/z = 304 $[M + H]^+$, 325 $[M + Na]^+$.

General Procedure for the Preparation of 6-[1-(2,6-Dihalophenyl)ethyl]-2-thioxo-2,3-dihydropyrimidin-4(1*H*)-ones (12, 13, and 14). Example: 6-(1-(2,6-Difluorophenyl)-ethyl)-5-methyl-2-thioxo-2,3-dihydropyrimidin-4(1*H*)-one 14. To a stirred solution of sodium metal (0.06 g, 2.7 mmol) in dry EtOH (5 mL) under Ar atmosphere thiourea (0.15 g, 1.9 mmol) was added, and the mixture was stirred at room temperature until complete dissolution. A solution of **11** (0.40 g, 1.3 mmol) in dry EtOH (15 mL) was added dropwise, and the mixture was stirred at reflux for 12 h. Solvent was evaporated and the residue treated with H_2O and neutralized with AcOH 0.5 N. The aqueous phase was extracted with EtOAc (3 × 30 mL), dried over Na_2SO_4, filtered, and concentrated under reduced pressure. The crude residue was recrystallized from EtOH to give compound **14** as a white solid (isolated yield 65%). ^{1}H NMR (400 MHz DMSO) δ ppm 11.59 (s, 1H), 7.46−7.29 (m, 1H), 7.08 (t, J = 8.6 Hz, 2H), 4.47 (q, J = 7.3 Hz, 1H), 1.61 (d, J = 7.3 Hz, 3H), 1.55 (s, 3H). LRMS (ESI) m/z = 305 $[M + Na]^+$, 283 $[M + H]^+$.

6-(1-(2,6-Dichlorophenyl)ethyl)-2-mercaptopyrimidin-4(3*H*)-one 12. ^{1}H NMR (400 MHz DMSO) δ ppm 9.44 (bs, 1H), 8.40 (bs, 1H), 7.45−7.25 (m, 3H), 4.18 (s, 1H), 2.09 (s, 3H). LRMS (ESI) m/z = 302 $[M + H]^+$.

6-(1-(2,6-Dichlorophenyl)ethyl)-2-mercapto-5-methylpyrimidin-4(3*H*)-one 13. ^{1}H NMR (400 MHz DMSO) δ ppm 12.50 (s, 1H), 10.99 (s, 1H), 7.48−7.43 (m, 2H), 7.31 (t, J = 8.0, Hz, 1H), 4.35−4.76 (m, 1H), 1.56 (d, J = 7.6 Hz, 3H), 1.36 (s, 3H). LRMS (ESI) m/z = 315 $[M + H]$+.

General Procedure for the Preparation of 6-[1-(2,6-Dihalophenyl)ethyl]-2-(methylthio)pyrimidin-4(3*H*)-ones (14−17). Example: 6-(1-(2,6-Difluorophenyl)ethyl)-5-methyl-2-(methylthio)pyrimidin-4(3*H*)-one 17. To a stirred solution of KOH (0.01 g, 0.16 mmol) in EtOH (2 mL) **14** (0.05 g, 0.16 mmol) was added, and the mixture was stirred at room temperature until complete dissolution. Iodomethane (0.01 mL, 0.16 mmol) was added dropwise, and the mixture was stirred at room temperature for 1 h. Solvent was evaporated and the residue dissolved in EtOAc (20 mL) and washed with H_2O (2 × 15 mL). The organic phase was dried over Na_2SO_4, filtered, and concentrated under reduced pressure. The crude residue was purified by flash chromatography on silica gel, eluting with 40% EtOAc/Hex to give pure compound **17** (isolated yield 95%). ^{1}H NMR (400 MHz DMSO) δ ppm 7.36−7.23 (m, 1H), 7.00 (m, 2H), 4.52 (q, J = 7.1 Hz, 1H), 2.36 (s, 3H), 1.82 (s, 3H), 1.56 (d, J = 7.1 Hz, 3H). LRMS (ESI) m/z = 319 $[M + Na]^+$, 297 $[M + H]^+$.

6-(1-(2,6-Dichlorophenyl)ethyl)-5-methyl-2-(methylthio)-pyrimidin-4(3*H*)-one 15. Yield 94%, white solid. ^{1}H NMR (400 MHz, $CDCl_3$) δ ppm 7.24 (d, J = 8.0 Hz, 2H), 7.07 (t, J = 8.0 Hz, 1H), 4.92−4.87 (m, 1H), 2.59 (s, 3H), 1.65 (s, 3H), 1.63 (s, 3H). LRMS (ESI) m/z = 329 $[M + H]^+$.

6-(2,6-Dichlorobenzyl)-5-methyl-2-(methylthio)pyrimidin-4(3*H*)-one 16. Yield 98%, white solid. ^{1}H NMR (400 MHz, $CDCl_3$) δ ppm 7.30−7.10 (m, 3H), 4.22 (s, 2H), 2.17 (s, 3H), 2.15 (s, 3H). LRMS (ESI) m/z = 316 $[M + H]^+$.

General Procedure for the Preparation of 6-(1-(2,6-Dihalophenyl)ethyl)-5-methyl-2-(methylsulfonyl)pyrimidin-4(3*H*)-ones (18−20). Example: 6-(1-(2,6-Difluorophenyl)ethyl)-5-methyl-2-(methylsulfonyl)pyrimidin-4(3*H*)-one 20. To a stirred solution of **17** (0.03 g, 0.10 mmol) in dry DCM (5 mL) at 0 °C, 3-chloroperbenzoic acid (0.05 g, 0.25 mmol) was added, and the mixture was stirred at 0 °C for 1 h and then at room temperature for 12 h. The reaction was quenched with a saturated solution of $NaHCO_3$ (5 mL) and extracted with EtOAc (3 × 10 mL). The organic phase was dried over Na_2SO_4, filtered, and concentrated under reduced pressure. The crude residue was purified by flash chromatography on silica gel, eluting with 2% MeOH/DCM to give pure compound **20** (isolated yield 63%). ^{1}H NMR (400 MHz, $CDCl_3$) δ ppm 7.23−7.10 (m, 1H), 6.83 (t, J = 8.4 Hz, 2H), 4.68 (q, J = 7.1 Hz, 1H), 3.29 (s, 3H), 2.09 (s, 3H), 1.69 (d, J = 7.1 Hz, 3H). LRMS (ESI) m/z = 351 $[M + Na]^+$, 329 $[M + H]^+$.

6-(2,6-Dichlorobenzyl)-5-methyl-2-(methylsulfonyl)-pyrimidin-4(3*H*)-one 18. Yield 63%, white solid. ^{1}H NMR (400 MHz, $CDCl_3$) δ ppm 7.30−7.10 (m, 3H), 4.22 (s, 2H), 2.17 (s, 3H), 2.15 (s, 3H). LRMS (ESI) m/z = 349 $[M + H]^+$.

6-(1-(2,6-Dichlorophenyl)ethyl)-5-methyl-2-(methylsulfonyl)pyrimidin-4(3*H*)-one 19. Yield 65%, white solid. ^{1}H NMR (400 MHz, $CDCl_3$) δ ppm 7.25(d, J = 8.0 Hz, 2H), 7.10 (t, J = 8.0 Hz, 1H), 5.10 (q, J = 6.8 Hz, 1H), 3.30 (s, 3H), 1.73 (s, 3H), 1.69 (d, J = 6.8 Hz, 3H). LRMS (ESI) m/z = 362 $[M + H]^+$.

***tert*-Butyl Piperazine-1-carboxylate (26b).** Piperazine (100 mg, 1.61 mmol) and di-*tert*-butyl dicarbonate $[(Boc)_2O]$ (386 mg, 1.71 mmol) were suspended in MeOH (2 mL) in a 10 mL glass vial equipped with a small magnetic stirring bar. The mixture was irradiated for 2 min at 100 °C using an irradiation power of 300 W. The reaction was monitored using TLC. After that time, cold water was added (10 mL), and the reaction mixture was extracted with EtOAc (3 × 5 mL). The organic phase was washed with brine, dried over Na_2SO_4, filtered, and concentrated under reduced pressure. The resulting residue was purified by flash chromatography (MeOH/EtOAc 1:5). Yield 86%, white solid. ^{1}H NMR (400 MHz, $CDCl_3$) δ (ppm) 3.35−3.33 (m, 4H), 2.77−2.75 (m, 4H), 2.03 (bs, 1H), 1.41 (s, 9H). LRMS (ESI) m/z: 187 $[M + H]^+$.

General Procedure for the Preparation of Aminobenzaldehydes (21b−d). Example: *tert*-Butyl 4-(4-Formylphenyl)-piperazine-1-carboxylate (21b). 4-Fluorobenzaldehyde (266 mg, 2.14 mmol), *tert*-butyl 4-(4-formylphenyl)piperazine-1-carboxylate (400 mg, 2.14 mmol, K_2CO_3, 296 mg, 4.28 mmol) were stirred in dry DMF at 130 °C under nitrogen atmosphere. After 12 h, the reaction was quenched by addition of water. The resulting mixture was extracted with EtOAc (3 × 25 mL), washed with brine, and dried over anhydrous Na_2SO_4. The resulting residue was purified by flash chromatography (PE/EtOAc 4:1). Yield 65%, white solid. ^{1}H NMR (400 MHz, $CDCl_3$) δ (ppm) 9.75 (s, 1H), 7.73 (d, J = 8.1 Hz, 2H), 6.87 (d, J = 8.1 Hz, 2H), 3.57−3.55 (m, 4H), 3.37−3.34 (m, 4H), 1.46 (s, 9H). LRMS (ESI) m/z: 291 $[M + H]^+$.

4-Morpholinobenzaldehyde (21c). Yield 99%, yellow solid. ^{1}H NMR (400 MHz, $CDCl_3$) δ (ppm) 9.79 (s, 1H), 7.76 (d, J = 8.0 Hz, 2H), 6.91 (d, J = 8.0 Hz, 2H), 3.84−3.82 (m, 4H), 3.33−3.31 (m, 4H). LRMS (ESI) m/z: 192 $[M + H]^+$.

4-(4-Methylpiperazin-1-yl)benzaldehyde (21d). Yield 95%, yellow solid. ^{1}H NMR (400 MHz, $CDCl_3$) δ (ppm) 9.76 (s, 1H), 7.72 (d, J = 8.0 Hz, 2H), 6.90 (d, J = 8.0 Hz, 2H), 3.41−3.39 (m, 4H), 2.55−2.53 (m, 4H), 2.34 (s, 3H). LRMS (ESI) m/z: 205 $[M + H]^+$.

General Procedure for the Preparation of 1-(Aralkyl)-*N*-methylmethanamines (22b−g). Example: 1-(1*H*-Indazol-3-yl)-*N*-methylmethanamine 22g. A 40% aqueous solution of methylamine (0.16 mL, 2.05 mmol) was diluted with MeOH (8 mL). 1*H*-Indazole-3-carboxaldehyde (0.10 g, 0.69 mmol) and $NaHCO_3$ (0.03 g, 0.82 mmol) were added. The mixture was stirred at reflux for 4 h. Then it was cooled to 0 °C and $NaBH_4$ (0.12 g, 1.37 mmol) was added and the mixture was stirred at room temperature for 1 h. The reaction was quenched with H_2O (10 mL) and extracted with EtOAc (3 × 5 mL). The organic phase was dried over Na_2SO_4, filtered, and concentrated under reduced pressure. The crude residue was purified by flash chromatography on silica gel, eluting with a 0.5/1/9 mixture of TEA/MeOH/DCM to give pure compound **22g** (isolated yield 52%). ^{1}H NMR (400 MHz, $CDCl_3$) δ ppm 7.68 (d, J = 8.0 Hz, 1H), 7.33 (d, J = 8.3 Hz, 1H), 7.24 (t, J = 7.4 Hz, 1H), 7.04 (t, J = 7.3 Hz, 1H), 4.15 (s, 2H), 2.47 (s, 3H). LRMS (ESI) m/z = 162 $[M + H]^+$.

***tert*-Butyl 4-(4-((Methylamino)methyl)phenyl)piperazine-1-carboxylate (22b).** Yield 90%, foam. ^{1}H NMR (400 MHz, $CDCl_3$)

DOI: 10.1021/acs.jmedchem.5b01979
J. Med. Chem. XXXX, XXX, XXX−XXX

δ (ppm) 7.23 (d, J = 8.0 Hz, 2H), 6.88 (d, J = 8.0 Hz, 2H), 4.80 (s, 1H), 3.73 (s, 2H), 3.56−3.54 (m, 4H), 3.11−3.09 (m, 4H), 2.42 (s, 3H), 1.47 (s, 9H). LRMS (ESI) m/z: 306 $[M + H]^+$.

***N*-Methyl-1-(4-morpholinophenyl)methanamine (22c).** Yield 95%, light yellow oil. ^{1}H NMR (400 MHz, $CDCl_3$) δ (ppm) 9.79 (s, 1H), 7.11 (d, J = 8.3 Hz, 2H), 6.75 (d, J = 8.3 Hz, 2H), 3.86−3.84 (m, 4H), 3.55 (s, 2H), 3.14−3.12 (m, 4H), 2.29 (s, 3H). LRMS (ESI) m/z: 207 $[M + H]^+$.

***N*-Methyl-1-(4-(4-methylpiperazin-1-yl)phenyl)-methanamine (22d).** Yield 70%, yellow solid. ^{1}H NMR (400 MHz, $CDCl_3$) δ (ppm) 7.10 (d, J = 8.0 Hz, 2H), 6.78 (d, J = 8.0 Hz, 2H), 3.54 (s, 2H), 3.09−3.07 (m, 4H), 2.46−2.44 (m, 4H), 2.34 (s, 3H). LRMS (ESI) m/z: 220 $[M + H]^+$.

(4-Methoxyphenyl)-*N*-methylmethanamine (22e). Yield 97%, colorless oil. ^{1}H NMR (400 MHz, $CDCl_3$) δ (ppm) 7.13−7.11 (d, 2H, J = 8.3 Hz), 6.77−6.75 (d, 2H, J = 8.3 Hz), 3.67 (s, 3H), 3.57 (s, 2H), 2.32 (s, 3H). LRMS (ESI) m/z: 152 $[M + H]^+$.

***N*-Methyl-1-(4-nitrophenyl)methanamine (22f).** Yield 95%, orange solid. ^{1}H NMR (400 MHz, $CDCl_3$) δ (ppm) 8.17 (d, J = 8.6 Hz, 2H,), 7.49 (d, J = 8.6 Hz, 2H), 3.85 (s, 2H), 2.46 (s, 3H). LRMS (ESI) m/z: 167 $[M + H]^+$.

General Procedure for the Preparation of 2-(((1*H*-Indazol-3-yl)methyl)(methyl)amino)-6-(1-(2,6-difluorophenyl)ethyl)-5-methylpyrimidin-4(3*H*)-ones. Example: 2-(((1*H*-Indazol-3-yl)-methyl)(methyl)amino)-6-(1-(2,6-difluorophenyl)ethyl)-5-methylpyrimidin-4(3*H*)-one 25g. To stirred solution of **19** (0.03 g, 0.17 mmol) in dry toluene (5 mL) **22g** (0.02 g, 0.06 mmol) was added, and the mixture was stirred at reflux for 48 h. After cooling, the mixture was diluted with MeOH and evaporated under reduced pressure. The crude residue was purified by flash chromatography on silica gel, eluting with 5% MeOH/DCM to give pure compound **25g** (isolated yield 60%). ^{1}H NMR (400 MHz, $CDCl_3$) δ ppm 7.47 (dd, J = 7.8, 5.8 Hz, 2H), 7.41−7.30 (m, 1H), 7.12−6.96 (m, 2H), 6.75 (t, J = 8.3 Hz, 2H), 5.21 (d, J = 15.3 Hz, 1H CH-N), 4.96 (d, J = 15.3 Hz, 1H CH-N), 4.58 (q, J = 7.1 Hz, 1H), 3.05 (s, 3H), 1.93 (s, 3H), 1.65 (d, J = 7.1 Hz, 3H). ^{13}C NMR (100 MHz, $CDCl_3$) δ ppm 165.97, 165.52, 151.45, 142.43, 127.69, 126.97, 121.37, 120.88, 120.32, 111.37, 111.13, 109.95, 106.16, 45.13, 34.28, 17.60, 9.35, 5.45. LRMS (ESI) m/z = 432 $[M + Na]^+$, 410 $[M + H]^+$.

6-(2,6-Dichlorobenzyl)-2-((4-methoxybenzyl)(methyl)-amino)-5-methylpyrimidin-4(3*H*)-one (23e). The residue was crystallized from EtOH. Yield 57%. White solid. ^{1}H NMR (400 MHz, $CDCl_3$) δ ppm 9.48 (s, 1H), 7.25 (d, J = 8.0 Hz, 2H), 7.04 (t, J =7.8 Hz, 1H), 6.88 (d, J = 8.0 Hz, 2H), 6.72−6.70 (m, 2H), 4.35 (s, 2H), 4.17 (s, 2H), 3.77 (s, 3H), 2.86 (s, 3H), 2.08 (s, 3H). ^{13}C NMR (100 MHz, $CDCl_3$) δ ppm 158.72, 135.90, 135.73, 129.91, 129.67, 128.98, 128.19, 113.84, 55.32, 50.99, 35.89, 34.24, 16.21, 10.08. LRMS (ESI) m/z = 419 $[M + H]^+$.

6-(1-(2,6-Dichlorophenyl)ethyl)-2-((4-methoxybenzyl)-(methyl)amino)-5-methylpyrimidin-4(3*H*)-one (24e). The residue was purified by flash chromatography (DCM/MeOH 99:1). Yield 57%. White solid. ^{1}H NMR (400 MHz, $CDCl_3$) δ ppm 11.48 (s, 1H), 7.24 (d, J = 8.0 Hz, 2H), 7.19 (d, J = 8.0 Hz, 2H), 7.08−7.05 (m, 1H), 6.83 (d, J = 8.0 Hz, 2H), 6.92 (q, J = 7.3 Hz, 1H), 4.81 (m, 1H), 4.63 (m, 1H), 3.78 (s, 1H), 3.06 (s, 3H), 1.58 (d, J = 7.2 Hz, 3H), 3.06 (s, 3H), 1.58 (s, 3H), 1.51 (s, 3H). ^{13}C NMR (100 MHz, $CDCl_3$) δ ppm158.72, 135.90, 135.73, 129.91, 129.67, 128.98, 113.84, 55.32, 50.99, 35.89, 34.24, 16.21, 15.68, 10.08. LRMS (ESI) m/z = 433 $[M + H]^+$.

6-(1-(2,6-Dichlorophenyl)ethyl)-5-methyl-2-(methyl(4-morpholinobenzyl)amino)pyrimidin-4(3*H*)-one (24c). The residue was purified by flash chromatography (DCM/MeOH 95:5). Yield 62%, white solid. ^{1}H NMR (400 MHz, $CDCl_3$) δ ppm 7.27−7.02 (m 3H), 7.20−7.18 (d, J = 8.0 Hz, 2H), 6.98−6.96 (J = 8.0 Hz, 2H), 4.84−4.78 (q, J = 8.0 Hz, 1H), 4.94−4.59 (m, 2H), 3.85 (t, J = 4.0 Hz, 4H), 3.14 (t, J = 4.0 Hz, 4H), 3.06 (s, 3H), 1.55 (d, J = 7.1 Hz, 3H), 1.51 (s, 3H). ^{13}C NMR (100 MHz, $CDCl_3$) δ ppm 161.5, 152.3, 150.4, 147.9, 141.0, 134.4, 128.8, 127.7, 126.8, 125.9, 122.7, 112.7, 66.3, 53.3, 52.3, 33.4, 18.1, 9.7. LRMS (ESI) m/z = 509 $[M + Na]^+$, 487 $[M + H]^+$.

6-(1-(2,6-Dichlorophenyl)ethyl)-5-methyl-2-(methyl(4-morpholinobenzyl)amino)pyrimidin-4(3*H*)-one (23c). The residue was purified by flash chromatography (DCM/MeOH 99:1). Yield 65%. White solid. ^{1}H NMR (400 MHz, $CDCl_3$) δ ppm 10.59 (s, 1H), 7.23 (d, J = 8.0 Hz, 2H), 7.03 (t, J = 7.9 Hz, 1H), 6.88 (d, J = 8.0 Hz, 2H), 6.73 (d, J = 8.0 Hz, 2H), 4.34 (s, 2H), 4.16 (s, 2H), 3.84 (t, J = 4.0 Hz, 4H), 3.11 (t, J = 4.0 Hz, 4H), 2.89 (s, 3H), 2.04 (s, 3H). ^{13}C NMR (100 MHz, $CDCl_3$) δ ppm 158.72, 145.90, 135.73, 129.91, 129.67, 128.98, 113.84, 71.45, 58.91, 55.32, 50.99, 35.89, 34.24, 16.21, 10.08. LRMS (ESI) m/z = 474 $[M + H]^+$.

6-(2,6-Dichlorobenzyl)-5-methyl-2-(methyl(4-(4-methylpiperazin-1-yl)benzyl)amino)pyrimidin-4(3*H*)-one (23d). The residue was purified by flash chromatography (DCM/MeOH 99:1). Yield 85%. White solid. ^{1}H NMR (400 MHz, $CDCl_3$) δ ppm 10.50 (bs 1H), 7.25(d, J = 8.0 Hz, 2H), 7.03(d, J = 8.0 Hz, 2H), 7.22−6.73 (m, 3H), 4.34 (s, 2H), 4.23 (s, 2H), 3.19−3.17 (t, J = 4.0 Hz, 4H), 2.83 (s, 3H), 2.58 (t, J = 4.0 Hz, 4H), 2.31 (s, 3H), 1.98 (s, 3H). ^{13}C NMR (100 MHz, $CDCl_3$) δ ppm 161.5, 152.3, 147.9, 145.8, 138.5, 135.7, 128.8, 127.5, 126.8, 125.9, 123.5, 57.2, 52.3, 52.2, 52.0, 46.6, 33.4, 20.1, 9.4. LRMS (ESI) m/z = 486 $[M + H]^+$, 508 $[M + Na]^+$.

6-(1-(2,6-Dichlorophenyl)ethyl)-5-methyl-2-(methyl(4-(4-methylpiperazin-1-yl)benzyl)amino)pyrimidin-4(3*H*)-one (24d). The residue was purified by flash chromatography (DCM/MeOH 95:5). Yield 60%. White solid. ^{1}H NMR (400 MHz, $CDCl_3$) δ ppm 7.24−7.02 (m, 3H), 7.16 (d, J = 8.0 Hz, 2H), 6.84 (d, J = 8.0 Hz, 2H), 4.91−4.57 (m, 2H), 4.83−4.80 (q, J =4.0 Hz, 1H), 3.21 (t, J = 4.0 Hz, 4H), 3.04 (s, 3H), 2.60 (t, J = 4.0 Hz, 4H), 2.36 (s, 3H), 1.58 (t, J = 8.0 Hz, 3H), 1.51 (s, 3H). ^{13}C NMR (100 MHz, $CDCl_3$) δ ppm 166.0, 165.4, 151.3, 150.4, 139.9, 135.2, 129.2, 116.2, 115.8, 115.5, 106.4, 55.0, 49.3, 48.9, 48.6, 46.0, 34.4, 16.0, 9.3. LRMS (ESI) m/z = 500 $[M + H]^+$, 522 $[M + Na]^+$.

***tert*-Butyl 4-(4-(((4-(2,6-Dichlorobenzyl)-5-methyl-6-oxo-1,6-dihydropyrimidin-2-yl)(methyl)amino)methyl)phenyl)-piperazine-1-carboxylate (23b).** The residue was purified by flash chromatography (DCM/MeOH 95:5). Yield 65%. White solid. ^{1}H NMR (400 MHz, $CDCl_3$) δ ppm 10.56 (bs, 1H), 7.25−7.02 (m, 3H), 6.99−6.73 (m, 4H), 4.34 (s, 2H), 3.56−3.54 (m, 4H), 3.08−3.06 (m, 4H), 2.89 (s, 3H), 2.04 (s, 3H), 1.47 (s, 9H). ^{13}C NMR (100 MHz, $CDCl_3$) δ ppm 165.5, 161.6, 154.7, 152.3, 151.5, 150.6, 136.4, 135.9, 129.2, 127.6, 116.4, 112.7, 106.2, 79.9, 51.8, 49.4, 36.1, 34.1, 8.4, 9.7, 9.4. LRMS (ESI) m/z = 573 $[M + H]^+$.

6-(2,6-Dichlorobenzyl)-5-methyl-2-(methyl(4-(piperazin-1-yl)benzyl)amino)pyrimidin-4(3*H*)-one 2,2,2-Trifluoroacetate (23a). The residue was crystallized from ethanol. Yield 95%. White solid. ^{1}H NMR (400 MHz, $CDCl_3$) δ ppm 10.42 (bs, 1H), 7.24−7.09 (m, 3H), 6.89−6.62 (m, 4H), 4.77 (s, 2H), 4.27 (s, 2H), 3.52−3.49 (m, 4H), 2.88−2.95 (m, 4H), 2.89 (s, 3H), 1.94 (s, 3H). ^{13}C NMR (100 MHz, $CDCl_3$) δ ppm 165.0, 165.4, 150.9, 150.2, 140.2, 136.1, 128.6, 115.7, 115.5, 106.4, 55.0, 49.3, 48.9, 48.6, 46.4, 9.1. LRMS (ESI) m/z = 472 $[M + H]^+$, 495 $[M + Na]^+$.

***tert*-Butyl 4-(4-(((4-(1-(2,6-Dichlorophenyl)ethyl)-5-methyl-6-oxo-1,6-dihydropyrimidin-2-yl)(methyl)amino)methyl)-phenyl)piperazine-1-carboxylate (24b).** The residue was purified by flash chromatography (DCM/MeOH 95:5). Yield 65%. White solid. ^{1}H NMR (400 MHz, $CDCl_3$) δ ppm 7.36−7.31 (m, 3H), 7.15 (d, J = 8.0 Hz, 2H), 6.92 (d, J = 8.0 Hz, 2H),), 5.07 (q, J = 8.0 Hz, 1H), 4.96 (d, J = 15.1 Hz, 1H CH-N), 4.59 (d, J = 15.1 Hz, 1H CH-N), 3.52−3.50 (m, 4H), 3.04−3.02 (m, 4H), 2.89 (s, 3H), 1.89 (s, 3H), 1.56 (d, J = 8.0 Hz, 3H), 1.47 (s, 9H) ppm. ^{13}C NMR (100 MHz, $CDCl_3$) δ ppm 165.5, 161.6, 154.7, 152.3, 151.5, 150.6, 136.4, 135.9, 129.2, 127.6, 116.4, 112.7, 106.2, 79.9, 51.8, 49.4, 36.1, 34.1, 8.4, 9.7, 9.4. 164.8, 160.6, 153.1, 152.7, 151.9, 151.6, 137.4, 135.9, 129.2, 128.6, 117.3, 113.7, 107.1, 80.0, 51.6, 48.1, 36.0, 34.3, 18.2, 8.6, 9.9, 9.3. LRMS (ESI) m/z = 586 $[M + H]^+$, 608 $[M + Na]^+$.

6-(1-(2,6-Dichlorophenyl)ethyl)-5-methyl-2-(methyl(4-(piperazin-1-yl)benzyl)amino)pyrimidin-4(3*H*)-one 2,2,2-Trifluoroacetate (24a). The residue was crystallized from ethanol. Yield 95%. White solid. ^{1}H NMR (400 MHz, $CDCl_3$) δ ppm ^{1}H NMR (400 MHz, $CDCl_3$) δ ppm 7.23−7.01 (m, 3H), 7.15 (d, J = 8.0 Hz, 2H), 6.82 (d, J = 8.0 Hz, 2H),), 4.91−4.57 (m, 2H), 4.82 (q, J = 8.0 Hz, 1H), 3.52−3.50 (m, 4H), 3.04−3.02 (m, 4H), 2.89 (s, 3H), 1.89 (s,

DOI: 10.1021/acs.jmedchem.5b01979
J. Med. Chem. XXXX, XXX, XXX−XXX

3H), 1.56 (d, J = 8.0 Hz, 3H) ppm. ^{13}C NMR (100 MHz, $CDCl_3$) δ ppm 165.5, 161.6, 161.2, 152.3, 151.5, 150.6, 136.4, 135.9, 129.2, 127.6, 116.4, 112.7, 106.2, 51.8, 49.4, 36.1, 34.1, 8.4, 9.7, 9.4. 164.8, 160.6, 153.1, 152.7, 151.9, 151.6, 137.4, 135.9, 129.2, 128.6, 117.3, 115.9, 113.7, 107.1, 80.0, 51.6, 48.1, 36.0, 18.2, 8.6, 9.9, 9.3. LRMS (ESI) m/z = 486 $[M + H]^+$, 508 $[M + Na]^+$.

6-(1-(2,6-Dichlorophenyl)ethyl)-5-methyl-2-(methyl(4-nitrobenzyl)amino)pyrimidin-4(3*H*)-one (24f). The residue was purified by flash chromatography (DCM/MeOH 95:5). Yield 40%. White solid. ^{1}H NMR (400 MHz, $CDCl_3$) δ ppm 8.16 (d, J = 8.0 Hz, 2H), 7.40 (d, J = 8.0 Hz, 2H), 7.24−7.20 (m, 2H), 7.04 (t, J = 8.0 Hz, 1H), 5.12−4.78 (m, 1 H), 3.43 (s, 2H), 3.14 (s, 3H), 1.55 (s, 3H), 1.51−1.48 (m, 3H). ^{13}C NMR (100 MHz, $CDCl_3$) δ ppm 162.3, 156.6, 152.1, 146.2, 142.5, 141.1, 135.5, 129.0, 127.9, 127.0, 124.2, 123.0, 55.1, 36.5, 35.0, 21.1, 14.2. LRMS (ESI) m/z = 448 $[M + H]^+$.

6-(1-(2,6-Difluorophenyl)ethyl)-5-methyl-2-(methyl(4-nitrobenzyl)amino)pyrimidin-4(3*H*)-one (25f). The residue was purified by flash chromatography (DCM/MeOH 95:5). Yield 64%. White solid. ^{1}H NMR (400 MHz, $CDCl_3$) δ ppm 8.10 (d, J =8.0 Hz, 2H), 7.31−7.26 (m, 2H), 7.09−7.03 (m, 1H), 6.73 (t, J = 8.0 Hz, 1H), 5.09 (d, J = 15.3 Hz, 1H CH-N), 4.62 (d, J = 15.3 Hz, 1H CH-N), 4.53 (q, J = 8.0 Hz, 3H), 3.09 (s, 3H), 1.89 (s, 3H), 1.56 (d, J = 7.1 Hz, 3H). ^{13}C NMR (100 MHz, $CDCl_3$) δ ppm 163.38, 163.38, 161.49, 155.86, 147.59, 144.57, 130.19, 128.29, 128.29, 123.78, 123.78, 122.27, 113.52, 112.06, 112.06, 57.42, 38.24, 38.01, 21.95, 13.66. LRMS (ESI) m/z = 400 $[M + H]^+$.

6-(1-(2,6-Difluorophenyl)ethyl)-2-((4-methoxybenzyl)-(methyl)amino)-5-methylpyrimidin-4(3*H*)-one (25e). The residue was purified by flash chromatography (DCM/MeOH 95:5). Yield 60%. White solid. ^{1}H NMR (400 MHz, $CDCl_3$) δ ppm 7.10−7.08 (m, 3H), 6.79−6.75 (m, 4H), 6.82 (d, J = 8.0 Hz, 2H), 4.86 (d, J = 15.3 Hz, 1H CH-N), 4.55−4−52 (m, 3H), 2,76 (s, 3H), 3.00 (s, 3H), 1.86 (s, 3H), 1.62 (d, J = 7.1 Hz, 3H). ^{13}C NMR (100 MHz, $CDCl_3$) δ ppm 163.38, 163.38, 161.49, 159.18, 155.86, 130.19, 128.91, 128.91, 128.00, 122.27, 113.54, 113.54, 113.52, 112.06, 112.06, 57.42, 56.04, 38.24, 38.01, 21.95, 13.66. LRMS (ESI) m/z = 400 $[M + H]^+$.

Biology. *Cells.* The JC53-BL cell line, also known as the TZM-bl cell line (NIH AIDS Research and Reference Reagent Program, Germantown, USA), was used for the evaluation of anti-HIV-1 activity of the N-DABOs. TZM-bl cells were cultured in Dulbecco's minimum essential medium (DMEM) (Lonza) containing 10% heat-inactivated FBS and 50 μg of gentamycin/mL at 37 °C in a humidified 5% CO_2, 95% air environment. Twice a week the cells were treated with 0.25% trypsin−1 mM EDTA (Lonza) for 10 min. The resulting cell suspension was washed with an equivalent amount of TZM-bl medium and subsequently seeded in a T75 culture flask (Greiner Bio-One, Germany) at 10^6 cells in 20 mL of medium.

Antiviral Activity Assay. The antiviral activity of the newly designed compounds was measured by preincubating 10 000 TZM-bl cells (at 10^5 cells/mL in culture medium supplemented with 30 μg/mL DEAE dextran) in a 96-well plates for 30 min at 37 °C, 5% CO_2 in the presence or absence of serial dilutions of the respective compound. Subsequently, 200 $TCID_{50}$ of HIV-1 WT or mutant virus was added to each well and cultures were incubated for 48 h before quantifying luciferase activity, using a TriStar LB941 luminometer (Berthold Technologies GmbH & Co., KG, Bad Wildbad, Germany). Each condition was evaluated in triplicate wells and in at least two independent experiments. The antiviral activity of the compound was expressed as the percentage of viral inhibition compared to the untreated controls and subsequently plotted against the compound concentration. Nonlinear regression analysis was used to calculate the 50% effective concentration (EC_{50}) based on at least two independent measurements and using GraphPad Prism, version 5.03, for Windows (GraphPad Software, San Diego, CA, USA). The antiviral activity of the **25e** gel formulation was tested by the same procedure and in comparison with free **25e** in solution and the gel without compound (blank).

Antiviral Activity by Using a Transwell Assay. To avoid the antiviral effect of β-cyclodextrins and the toxic effect on monolayers of highly concentrated gels (toxicity was observed with the original preparation at 5% concentration), **25e** gel was reformulated without these additives and antiviral activity was investigated with a Transwell experiment. TZM-bl cells were plated at 4 × 10^4 cells/well into each Transwell apical chamber of a 24-well plate (pore size 3 μm and diameter 6.5 mm, Corning Costar). The insert was placed in the bottom plate, which contains cell culture medium and cultured overnight. NL4.3 HIV virus was titrated as follows: medium was removed from all wells, and 100 μL of blank gel was added to all the apical chambers. A serial dilution of NL4.3 stock virus was made and 100 μL was added in triplicate to the top chamber, while culture medium was added in the bottom compartment. After 72 h luciferase activity was quantified as above.

For efficacy testing, 60 $TCID_{50}$ of virus was added to each apical well in the presence of 100 μL of **25e** gel, tenofovir gel, or blank gel at the final drug concentrations of 5000, 500, 50, 5, and 0.5 nM. In all apical wells, gels were used at 50% concentration directly on monolayers, but cells were exposed to the culture medium present in the bottom plate. Inhibition was determined as previously based on deviations from blank gel.

Reverse Transcriptase Activity Assay. Chemicals. [^{3}H]dTTP (40 Ci/mmol) was from PerkinElmer, and unlabeled dTTP was from Promega. PerkinElmer was the supplier of the GF/C filters. All other reagents were of analytical grade and purchased from Merck or Sigma-Aldrich.

Polymerase Assay. The homopolymer poly(rA) (Pharmacia) was mixed at weight ratios in nucleotides of 10:1 to the oligomer oligo(dT)12−18 (Pharmacia) in 20 mM Tris-HCl (pH 8.0) containing 20 mM KCl and 1 mM EDTA, heated at 65 °C for 5 min, and then slowly cooled at room temperature. The coexpression vectors pUC12N/p66(His)/p51 with the wild-type or mutant forms of HIV-1 RT p66 were kindly provided by Dr. S. H. Hughes (NCI-Frederick Cancer Research and Development Center). Proteins were expressed in *Escherichia coli* and purified as described.[40] RNA-dependent DNA polymerase activity was assayed as follows: a final volume of 25 μL contained reaction buffer (50 mM Tris-HCl, pH 7.5, 1 mM DTT, 0.2 mg/mL BSA, 4% glycerol), 10 mM $MgCl_2$, 0.5 μg of poly(rA)/oligo(dT)10:1 (0.3 μM 3′-OH ends), 10 μM [^{3}H]dTTP (1 Ci/mmol), and 2−4 nM RT. Reactions were incubated at 37 °C for 20 min. Ten microliter aliquots were then spotted on glass fiber filters GF/C, which were immediately immersed in 5% ice-cold TCA. Filters were washed twice in 5% ice-cold TCA and once in ethanol for 5 min and dried. Acid-precipitable radioactivity was quantitated by scintillation counting (Trilux Perkinelmer).

Inhibition Assays. Inhibition assays were performed under the conditions described for the HIV-1 RT RNA-dependent DNA polymerase activity assay. Incorporation of radioactive dTTP into poly(rA)/oligo(dT) at different substrate (nucleic acid or dTTP) concentrations was monitored in the presence of increasing fixed amounts of inhibitor. Data were then plotted according to Lineweaver−Burke and Dixon. For inhibition constant (K_i) determination, an interval of inhibitor concentration between 0.2K_i and 5K_i was used.

WST-1 Cytotoxicity Assay. The water-soluble tetrazolium-1 (WST-1) cell proliferation assay is a colorimetric assay for the measurement of cell proliferation and viability. The assay is based on the cleavage of the tetrazolium salt WST-1 (4-[3-(4-iodophenyl)-2-(4-nitrophenyl)-2*H*-5-tetrazolio]-1,3-benzene disulfonate) to a formazan dye by a complex cellular mechanism. This bioreduction is largely dependent on the glycolytic production of NAD(P)H in viable cells. Therefore, the amount of formazan dye formed correlates directly to the number of viable cells in the culture and can be quantified by measuring the absorbance at 450 nm in a multiwell plate reader. The greater is the number of viable cells, the greater is the amount of formazan dye produced following the addition of WST-1. Cytotoxicity of each compound was evaluated using this WST-1 viability assay, according to the manufacturer's instructions (Roche, Vilvoorde, Belgium). Briefly, 10 000 TZM-bl cells were seeded in a 96-well plates and cultured for 2 days in the presence of a serial dilution of compound. After this 48 h exposure, cell proliferation reagent, WST-1, was added and absorbance at 450 nm was quantified after 90 min using a microplate reader (BioRad, Tokio, Japan). Each compound was tested in three replicate

DOI: 10.1021/acs.jmedchem.5b01979
J. Med. Chem. XXXX, XXX, XXX−XXX

wells and in at least two independent experiments. The percentage cell viability, compared to untreated controls, was plotted against the compound concentration, and nonlinear regression analysis was performed using GraphPad Prism, version 5.02, for Windows (GraphPad Software, San Diego, CA, USA) to calculate the 50% cytotoxic concentration (CC_{50}).

ADME Assay. Chemicals and Excipients. All solvents, L-α-phosphatidylcholine, 2-hydroxypropyl-β-cyclodextrin (2-HP-βCD), hydroxyethylcellulose (HEC), and propionic acid were from Sigma-Aldrich Srl (Milan, Italy). Dodecane was purchased from Fluka (Milan, Italy). Milli-Q quality water (Millipore, Milford, MA, USA) was used. Hydrophobic filter plates (MultiScreen-IP, Clear Plates, 0.45 μm diameter pore size), 96-well microplates, and 96-well UV-transparent microplates were obtained from Millipore (Bedford, MA, USA).

Parallel Artificial Membrane Permeability Assay (PAMPA). Donor solution (0.5 mM) was prepared by diluting 1 mM dimethylsulfoxide (DMSO) compound stock solution using two buffers: phosphate buffer (25 mM, pH 7.4) and acetate buffer (50 mM, pH 4.2). Filters were coated with 5 μL of a 1% (w/v) dodecane solution of phosphatidylcholine. Donor solution (150 μL) was added to each well of the filter plate. To each well of the acceptor plate was added an amount of 300 μL of solution (50% DMSO in phosphate buffer). All compounds were tested in three different plates on different days. The sandwich was incubated for 5 h at room temperature under gentle shaking. After the incubation time, the plates were separated, and samples were taken from both receiver and donor sides and analyzed using LC with UV detection at 280 nm.

LC analysis was performed with a Varian Prostar HPLC system (Varian Analytical Instruments, USA) equipped with a binary pump with a manual injection valve and model Prostar 325 UV−vis detector. Chromatographic separation was conducted using a Phenomenex Kinetex C18-100A column (150 mm × 4.6 mm, 5 μm particle size) at a flow rate of 0.6 mL/min with a mobile phase composed of 60% ACN/40% formic acid (0.1%) or 35% ACN/65% formic acid (0.1%) for compounds **23f**, **25e**, **23c**, **24c**, **23d**, **24d**, respectively.

Permeability (Pe) was calculated according to the following equation, from Reis et al.,[42] in order to obtain effective permeability values in cm/s,

$$\mathrm{Pe} = \frac{-\ln\left[1 - \frac{C_A(t)}{C_{eq}}\right]}{A\left(\frac{1}{V_D} + \frac{1}{V_A}\right)t}$$

where C_{eq} is the equilibrium concentration reported by the following formula:

$$C_{eq} = \frac{C_D(t)V_D + C_A(t)V_A}{V_D + V_A}$$

V_A is the volume in the acceptor well, V_D is the volume in the donor well (cm^3), A is the "effective area" of the membrane (cm^2), $C_A(t)$ is the compound concentration in acceptor well at time t, $C_D(t)$ is the compound concentration in donor well at time t, and t is the incubation time (s).

Water Solubility Assay. Each solid compound (1 mg) was added to 1 mL of phosphate buffer (25 mM, pH 7.4) or acetate buffer (50 mM, pH 4.2). The samples were shaken in a shaker bath at room temperature for 24−36 h. Each suspension was filtered through a 0.45 μm nylon filter (Acrodisc), and the solubilized compound was determined by LC−MS−MS assay. For each compound the determination was performed in triplicate. For the quantification the following was used: an LC−MS system consisting of a Varian apparatus (Varian Inc.) including a vacuum solvent degassing unit, two pumps (212-LC), a triple quadrupole MSD (model 320-LC) mass spectrometer with ES interface, and Varian MS Workstation System Control, version 6.9 software. Chromatographic separation was obtained using a Pursuit C18 column (50 mm × 2.0 mm) (Varian) with 3 μm particle size and gradient elution, with eluent A being ACN and eluent B consisting of an aqueous solution of formic acid (0.1%). The analysis started with 0% of eluent A, which was linearly increased up to 70% in 10 min, then slowly increased up to 98% up to 15 min. The flow rate was 0.3 mL/min, and injection volume was 5 μL. The instrument operated in positive mode, and parameters were the following: detector 1850 V, drying gas pressure 25.0 psi, desolvation temperature 300.0 °C, nebulizing gas 40.0 psi, needle 5000 V, and shield 600 V. Nitrogen was used as nebulizer gas and drying gas. Collision induced dissociation was performed using argon as the collision gas at a pressure of 1.8 mTorr in the collision cell. The transitions as well as the capillary voltage and the collision energy used for compound are summarized in Table 4.

Table 4. Chromatographic and MS Parameters (Monitored Transition, Collision Energy, Capillary Voltage, and Retention Time t_R) of the Selected Compounds

compd	transition (m/z)	collision energy (eV)	capillary voltage (V)	t_R (min)
23c	309.9	−17.5	10	12.9
	176.0	−32.0		
23d	309.8	−21.0	10	11.2
	253.8	−36.5		
24d	323.9	−25.0	38	11.6
	288.0	−35.0		
23f	261.8	−30.5	24	10.2
	206.0	−45.0		
25e	291.9	17.0	50	11.0
	120.8	25.0		

Quantification of the single compound was made by comparison with apposite calibration curves realized with standard solutions in methanol.

Solubility Assessment. The solubilizing capacity of formulation media was measured in the presence of 50% w/w of 2-HP-β-CD. Stock solution of compound **25e** (DMSO) was added to obtain a concentration of 20 μM in a final volume of 1 mL (DMSO did not exceed 2%). After sonication, the samples were shaken in a shaker bath at room temperature for 24 h to reach equilibrium conditions. Each pregel solution was analyzed before and after filtration by a 0.45 μm nylon filter (Acrodisc). The loaded compound was determined using LC−UV−MS method already described for the permeability.

Molecular Modeling. Protein Preparation. The reverse transcriptase three-dimensional coordinates were selected from the Protein Data Bank (PDB entry code 1RT2)[41] and was prepared by means of Protein Preparation Wizard workflow implemented in the Maestro suite.[42] In particular, the inhibitor and the water molecules were deleted, hydrogen atoms were added, and bond orders and charges were assigned; the orientation of hydroxyl groups on Ser, Thr, and Tyr, the side chains of Asn and Gln residues, and the protonation state of His residues were optimized. Steric clashes were relieved by performing a small number of minimization steps, not intended to minimize the system completely. In our study, the minimization (OPLS force field) was stopped when the rmsd of the non-hydrogen atoms reached 0.30 Å. The same procedure was applied to prepare the RT protein in complex with the water molecule making a bridge between the crystallized ligand TNK-651 and the amino acids Lys101 of chain A and Glu138 of chain B. In this case, the water molecule 1023 was kept in the system during the Protein Preparation Wizard workflow. To prepare the input structure for Autodock calculations, the RT structure was further manipulated by removing nonpolar hydrogen atoms, while Kollman united-atom partial charges and solvent parameter were added. Autogrid was then used to generate grid maps.

Ligand Preparation. 168 S-DABOs/N-DABOs were collected from previous work and were built with the Schrodinger Maestro 9.2 graphical interface.[42] Compounds were then processed with the Schrodinger LigPrep tool to generate separate files for all possible enantiomers and protonation states at phisiological pH. OPLS_2005 was used as force field. Ligands for Autodock were further refined by

DOI: 10.1021/acs.jmedchem.5b01979
J. Med. Chem. XXXX, XXX, XXX−XXX

deleting the nonpolar hydrogen atoms and adding Gasteiger atomic charges.

Docking Simulation. Docking studies were performed within the NNBP of RT using three software packages: Autodock,[28] Gold,[29] and Glide.[30,31] The reliability of the docking protocols was first checked by simulating the binding mode of known ligands for which the poses have been experimentally determined (TNK-651, MKC-442, and HEPT). The three docking algorithms were able to correctly predict the binding modes of the reference compounds. With regard to the Gold program, the ChemScore scoring function was found to be the best one in terms of pose prediction (in comparison with GoldScore, CHEMPLP, and ASP) and was thus used in the following calculations. The genetic algorithm parameter settings were employed using the search efficiency set at 100%, and 100 runs were carried out for each ligand. Finally, results differing less than 1 Å in ligand-all atom rmsd were clustered together. For each inhibitor, the first ranked solution was selected for further analysis. The Lamarckian genetic algorithm (LGA) was used in Autodock to explore the possible orientations/conformations of the inhibitors in the binding site. For each compound, the following protocol was applied: 50 independent LGA runs, a population size of 150 individuals, and a maximum number of 2 500 000 energy evaluations. Moving to the Glide software, compounds were docked and scored using the Glide Standard Precision (SP) mode.

Multiple Linear Regression. QSAR calculations were performed using Canvas implemented in Maestro (version 9.5).[42] The conformer of each inhibitor was extracted from the complex with RT and submitted to the calculation of both QikProp and 2D fingerprint descriptors. These calculated properties, together with the parameters previously derived from docking studies with three different software as well as with the rescoring methods employed (MM-GBSA, XSCORE), were used as dependent variables to generate multiple linear regression (MLR) models, while enzymatic or cellular data were in turn used as the independent variable (expressed as $-\log IC_{50}$ or $-\log EC_{50}$). In the case of chiral compounds, the 3D energetic parameters coming from docking studies were calculated as the medium of the values obtained with all the possible diastereomeric forms. Molecules together with the calculated descriptors were imported in the cheminformatics package Canvas, and a MLR was carried out. The Simulated Annealing algorithm of Canvas was applied to descriptors to efficiently search the wide solution space and to identify the best subsets of descriptors to build robust QSAR models. The number of Monte Carlo steps was set to 1000.

■ ASSOCIATED CONTENT

Supporting Information

The Supporting Information is available free of charge on the ACS Publications website at DOI: 10.1021/acs.jmedchem.5b01979.

2D structures of S-DABO/N-DABO used for molecular modeling analysis (PDF)

Molecular formula strings (CSV)

■ AUTHOR INFORMATION

Corresponding Author

*Phone: +39 0577 234306. Fax: +39 0577 234306.

Notes

The authors declare no competing financial interest.

■ ACKNOWLEDGMENTS

This work was supported by the European Union collaborative project "CHAARM" (Grant HEALTH-F3-2009-242135) and by the Italian Ministero dell'Istruzione, dell'Università e della Ricerca, Prin 2010 research project (Grant 2010W2KM5L). Tenofovir was obtained through the NIH AIDS Reagent Program, Division of AIDS, NIAID, NIH.

■ ABBREVIATIONS USED

cART, combination antiretroviral therapy; RTI, reverse transcriptase inhibitor; S-DABO, *S*-dihydroalkyloxybenzyloxopyrimidine; N-DABO, *N*-dihydroalkyloxybenzyloxopyrimidine; WST-1, 4-[3-(4-iodophenyl)-2-(4-nitrophenyl)-2*H*-5-tetrazolio]-1,3-benzene disulfonate; CDI, 1,1′-carbonyldiimidazole; LDA, lithium diisopropylamide; HEC, hydroxyethylcellulose

■ REFERENCES

(1) Looney, D.; Ma, A.; Johns, S. HIV therapy-the state of art. *Curr. Top. Microbiol. Immunol.* **2015**, *389*, 1−29.

(2) Franzetti, M.; Violin, M.; Antinori, A.; De Luca, A.; Ceccherini-Silberstein, F.; Gianotti, N.; Torti, C.; Bonora, S.; Zazzi, M.; Balotta, C. Trends and correlates of HIV-1 resistance among subjects failing an antiretroviral treatment over the 2003−2012 decade in Italy. *BMC Infect. Dis.* **2014**, *14*, 398.

(3) Zhan, P.; Liu, X.; Li, Z. Recent advances in the discovery and development of novel HIV-1 NNRTI platforms: 2006−2008 update. *Curr. Med. Chem.* **2009**, *16*, 2876−2889.

(4) Song, Y.; Fang, Z.; Zhan, P.; Liu, X. Recent advances in the discovery and development of novel HIV-1 NNRTI platforms (Part II): 2009−2013 update. *Curr. Med. Chem.* **2014**, *21*, 329−355.

(5) Manetti, F.; Esté, J. A.; Clotet-Codina, I.; Armand-Ugón, M.; Maga, G.; Crespan, E.; Cancio, R.; Mugnaini, C.; Bernardini, C.; Togninelli, A.; Carmi, C.; Alongi, M.; Petricci, E.; Massa, S.; Corelli, F.; Botta, M. Parallel solution-phase and microwave-assisted synthesis of new S-DABO derivatives endowed with subnanomolar anti-HIV-1 activity. *J. Med. Chem.* **2005**, *48*, 8000−8008.

(6) Mugnaini, C.; Manetti, F.; Esté, J. A.; Clotet-Codina, I.; Maga, G.; Cancio, R.; Botta, M.; Corelli, F. Synthesis and biological investigation of S-aryl-S-DABO derivatives as HIV-1 inhibitors. *Bioorg. Med. Chem. Lett.* **2006**, *16*, 3541−3544.

(7) Radi, M.; Contemori, L.; Castagnolo, D.; Spinosa, R.; Esté, J. A.; Massa, S.; Botta, M. A versatile route to C-6 arylmethyl-functionalized S-DABO and related analogues. *Org. Lett.* **2007**, *9*, 3157−3160.

(8) Mugnaini, C.; Alongi, M.; Togninelli, A.; Gevariya, H.; Brizzi, A.; Manetti, F.; Bernardini, C.; Angeli, L.; Tafi, A.; Bellucci, L.; Corelli, F.; Massa, S.; Maga, G.; Samuele, A.; Facchini, M.; Clotet-Codina, I.; Armand-Ugón, M.; Esté, J. A.; Botta, M. Dihydro-alkylthio-benzyloxopyrimidines as inhibitors of reverse transcriptase: synthesis and rationalization of the biological data on both wild-type enzyme and relevant clinical mutants. *J. Med. Chem.* **2007**, *50*, 6580−6595.

(9) Radi, M.; Falciani, C.; Contemori, L.; Petricci, E.; Maga, G.; Samuele, A.; Zanoli, S.; Terrazas, M.; Castria, M.; Togninelli, A.; Esté, J. A.; Clotet-Codina, I.; Armand-Ugón, M.; Botta, M. A multidisciplinary approach for the identification of novel HIV-1 nonnucleoside reverse transcriptase inhibitors: S-DABOCs and DAVPs. *ChemMedChem* **2008**, *3*, 573−593.

(10) Botta, M.; Corelli, F.; Petricci, E.; Radi, M.; Maga, G.; Estè, J. A.; Mai, A. WO/2007/043094, 2007.

(11) Radi, M.; Angeli, L.; Franchi, L.; Contemori, L.; Maga, G.; Samuele, A.; Zanoli, S.; Armand-Ugon, M.; Gonzalez, E.; Llano, A.; Esté, J. A.; Botta, M. Towards novel S-DABOC inhibitors: synthesis, biological investigation, and molecular modeling studies. *Bioorg. Med. Chem. Lett.* **2008**, *18*, 5777−5780.

(12) Radi, M.; Maga, G.; Alongi, M.; Angeli, L.; Samuele, A.; Zanoli, S.; Bellucci, L.; Tafi, A.; Casaluce, G.; Giorgi, G.; Armand-Ugon, M.; Gonzalez, E.; Esté, J. A.; Baltzinger, M.; Bec, G.; Dumas, P.; Ennifar, E.; Botta, M. Discovery of chiral cyclopropyl dihydro-alkylthio-benzyloxopyrimidine (S-DABO) derivatives as potent HIV-1 reverse transcriptase inhibitors with high activity against clinically relevant mutants. *J. Med. Chem.* **2009**, *52*, 840−851.

(13) Radi, M.; Pagano, M.; Franchi, L.; Castagnolo, D.; Schenone, S.; Casaluce, G.; Zamperini, C.; Dreassi, E.; Maga, G.; Samuele, A.; Gonzalo, E.; Clotet, B.; Esté, J. A.; Botta, M. Synthesis, biological activity, and ADME properties of novel S-DABOs/N-DABOs as HIV reverse transcriptase inhibitors. *ChemMedChem* **2012**, *7*, 883−896.

DOI: 10.1021/acs.jmedchem.5b01979
J. Med. Chem. XXXX, XXX, XXX−XXX

(14) Olsen, J. S.; Easterhoff, D.; Dewhurst, S. Advances in HIV microbicide development. *Future Med. Chem.* **2011**, *3*, 2101−2116.
(15) Ariën, K. K.; Venkatraj, M.; Michiels, J.; Joossens, J.; Vereecken, K.; Van der Veken, P.; Abdellati, S.; Cuylaerts, V.; Crucitti, T.; Heyndrickx, L.; Heeres, J.; Augustyns, K.; Lewi, P. J.; Vanham, G. Diaryltriazine non-nucleoside reverse transcriptase inhibitors are potent candidates for pre-exposure prophylaxis in the prevention of sexual HIV transmission. *J. Antimicrob. Chemother.* **2013**, *68*, 2038−2047.
(16) Fletcher, P.; Harman, S.; Azijn, H.; Armanasco, N.; Manlow, P.; Perumal, D.; de Béthune, M. P.; Nuttall, J.; Romano, J.; Shattock, R. Inhibition of human immunodeficiency virus type 1 infection by the candidate microbicide dapivirine, a nonnucleoside reverse transcriptase inhibitor. *Antimicrob. Agents Chemother.* **2009**, *53*, 487−495.
(17) Fernández-Romero, J. A.; Thorn, M.; Turville, S. G.; Titchen, K.; Sudol, K.; Li, J.; Miller, T.; Robbiani, M.; Maguire, R. A.; Buckheit, R. W.; Hartman, T. L.; Phillips, D. M. Carrageenan/MIV-150 (PC-815), a combination microbicide. *Sex. Transm. Dis.* **2007**, *34*, 9−14.
(18) Hossain, M. M.; Parniak, M. A. In vitro microbicidal activity of the nonnucleoside reverse transcriptase inhibitor (NNRTI) UC781 against NNRTI-resistant human immunodeficiency virus type 1. *J. Virol.* **2006**, *80*, 4440−4446.
(19) D'Cruz, O. J.; Uckun, F. M. Dawn of non-nucleoside inhibitor-based anti-HIV microbicides. *J. Antimicrob. Chemother.* **2006**, *57*, 411−423.
(20) Abdool Karim, Q.; Abdool Karim, S. S.; Frohlich, J. A.; Grobler, A. C.; Baxter, C.; Mansoor, L. E.; Kharsany, A. B.; Sibeko, S.; Mlisana, K. P.; Omar, Z.; Gengiah, T. N.; Maarschalk, S.; Arulappan, N.; Mlotshwa, M.; Morris, L.; Taylor, D. CAPRISA 004 Trial Group. Effectiveness and safety of tenofovir gel, an antiretroviral microbicide, for the prevention of HIV infection in women. *Science* **2010**, *329*, 1168−1174.
(21) Doncel, G. F.; Clark, M. R. Preclinical evaluation of anti-HIV microbicide products: new models and biomarkers. *Antiviral Res.* **2010**, *88* (Suppl. 1), S10−S18.
(22) Desai, M.; Iyer, G.; Dikshit, R. K. Antiretroviral drugs: critical issues and recent advances. *Indian J. Pharmacol.* **2012**, *44*, 288−298.
(23) Vanpouille, C.; Arakelyan, A.; Margolis, L. Microbicides: still a long road to success. *Trends Microbiol.* **2012**, *20*, 369−375.
(24) Pozzetto, B.; Delezay, O.; Brunon-Gagneux, A.; Hamzeh-Cognasse, H.; Lucht, F.; Bourlet, T. Current and future microbicide approaches aimed at preventing HIV infection in women. Expert Rev. *Expert Rev. Anti-Infect. Ther.* **2012**, *10*, 167−183.
(25) Selhorst, P.; Vazquez, A. C.; Terrazas-Aranda, K.; Michiels, J.; Vereecken, K.; Heyndrickx, L.; Weber, J.; Quiñones-Mateu, M. E.; Ariën, K. K.; Vanham, G. Human immunodeficiency virus type 1 resistance or cross-resistance to nonnucleoside reverse transcriptase inhibitors currently under development as microbicides. *Antimicrob. Agents Chemother.* **2011**, *55*, 1403−1413.
(26) Yang, H.; Parniak, M. A.; Isaacs, C. E.; Hillier, S. L.; Rohan, L. C. Characterization of cyclodextrin inclusion complexes of the anti-HIV non-nucleoside reverse transcriptase inhibitor UC781. *AAPS J.* **2008**, *10*, 606−613.
(27) Radi, M.; Evensen, L.; Dreassi, E.; Zamperini, C.; Caporicci, M.; Falchi, F.; Musumeci, F.; Schenone, S.; Lorens, J. B.; Botta, M. A combined targeted/phenotypic approach for the identification of new antiangiogenics agents active on a zebrafish model: from in silico screening to cyclodextrin formulation. *Bioorg. Med. Chem. Lett.* **2012**, *22*, 5579−5583.
(28) Morris, G. M.; Goodsell, D. S.; Halliday, R. S.; Huey, R.; Hart, W. E.; Belew, R. K.; Olson, A. J. Automated Docking Using a Lamarckian Genetic Algorithm and and Empirical Binding Free Energy Function. *J. Comput. Chem.* **1998**, *19*, 1639−1662.
(29) Verdonk, M. L.; Cole, J. C.; Hartshorn, M. J.; Murray, C. W.; Taylor, R. D. Improved Protein-Ligand Docking Using GOLD. *Proteins: Struct., Funct., Genet.* **2003**, *52*, 609−623.
(30) Halgren, T. A.; Murphy, R. B.; Friesner, R. A.; Beard, H. S.; Frye, L. L.; Pollard, W. T.; Banks, J. L. Glide: A New Approach for Rapid, Accurate Docking and Scoring. 2. Enrichment Factors in Database Screening. *J. Med. Chem.* **2004**, *47*, 1750−1759.
(31) Friesner, R. A.; Banks, J. L.; Murphy, R. B.; Halgren, T. A.; Klicic, J. J.; Mainz, D. T.; Repasky, M. P.; Knoll, E. H.; Shaw, D. E.; Shelley, M.; Perry, J. K.; Francis, P.; Shenkin, P. S. Glide: A New Approach for Rapid, Accurate Docking and Scoring. 1. Method and Assessment of Docking Accuracy. *J. Med. Chem.* **2004**, *47*, 1739−1749.
(32) Mai, A.; Artico, M.; Rotili, D.; Tarantino, D.; Clotet-codina, I.; Armand-Ugon, M.; Ragno, R.; Simeoni, S.; Sbardella, G.; Nawrozkij, M. B.; Samuele, A.; Maga, G.; Estè, J. A. Synthesis and biological properties of novel 2-aminopyrimidin-4(3*H*)-ones highly potent against HIV-1 mutant strains. *J. Med. Chem.* **2007**, *50*, 5412−5424.
(33) Rotili, D.; Samuele, A.; Tarantino, D.; Ragno, R.; Musmuca, I.; Ballante, F.; Botta, G.; Morera, L.; Pierini, M.; Cirilli, M.; Nawrozkij, M. B.; Gonzalez, E.; Clotet, B.; Artico, M.; Estè, J. A.; Maga, G.; Mai, A. 2-(Alkyl/aryl)amino-6-benzylpyrimidin-4(3*H*)-ones as inhibitors of wild-type and mutant HIV-1: enantioselectivity studies. *J. Med. Chem.* **2012**, *55*, 3558−3562.
(34) Wang, R.; Lai, L.; Wang, S. Further Development and Validation of Empirical Scoring Functions for Structure-Based Binding Affinity Prediction. *J. Comput.-Aided Mol. Des.* **2002**, *16*, 11−26.
(35) Genheden, S.; Ryde, U. The MM/PBSA and MM/GBSA methods to estimate ligand-binding affinities. *Expert Opin. Drug Discovery* **2015**, *10*, 449−461.
(36) Fraczek, T.; Siwek, A.; Paneth, P. Assessing molecular docking tools for relative biological activity prediction: a case study of triazole HIV-1 NNRTIs. *J. Chem. Inf. Model.* **2013**, *53*, 3326−3342.
(37) Jacobson, M. P.; Pincus, D. L.; Rapp, C. S.; Day, T. J. F.; Honig, B.; Shaw, D. E.; Friesner, R. A. A Hierarchical Approach to All-Atom Protein Loop Prediction. *Proteins: Struct., Funct., Genet.* **2004**, *55*, 351−367.
(38) Jacobson, M. P.; Friesner, R. A.; Xiang, Z.; Honig, B. On the Role of Crystal Packing Forces in Determining Protein Sidechain Conformations. *J. Mol. Biol.* **2002**, *320*, 597−608.
(39) Duan, J.; Dixon, S. L.; Lowrie, J. F.; Sherman, W. Analysis and comparison of 2D fingerprints: insights into database screening performance using eight fingerprint methods. *J. Mol. Graphics Modell.* **2010**, *29*, 157−170.
(40) Mai, A.; Sbardella, G.; Artico, M.; Ragno, R.; Massa, S.; Novellino, E.; Greco, G.; Lavecchia, A.; Musiu, C.; La Colla, M.; Murgioni, C.; La Colla, P.; Loddo, R. Structure-based design, synthesis, and biological evaluation of conformationally restricted novel 2-alkylthio-6-[1-(2,6-difluorophenyl)alkyl]-3,4-dihydro-5-alkyl-pyrimidin-4(3H)-ones as non-nucleoside inhibitors of HIV-1 reverse transcriptase. *J. Med. Chem.* **2001**, *44*, 2544−2554.
(41) Maga, G.; Amacker, M.; Ruel, N.; Hübscher, U.; Spadari, S. Resistance to nevirapine of HIV-1 reverse transcriptase mutants: loss of stabilizing interactions and thermodynamic or steric barriers are induced by different single amino acid substitutions. *J. Mol. Biol.* **1997**, *274*, 738−747.
(42) Reis, J. M.; Dezani, A. B.; Pereira, T. M.; Avdeef, A.; Serra, C. H. Lamivudine permeability study: a comparison between PAMPA, ex vivo and in situ Single-Pass Intestinal Perfusion (SPIP) in rat jejunum. *Eur. J. Pharm. Sci.* **2013**, *48*, 781−789.

DOI: 10.1021/acs.jmedchem.5b01979
J. Med. Chem. XXXX, XXX, XXX−XXX